

Cite this: *Nanoscale Adv.*, 2023, 5, 6787

# Molybdenum disulfide, exfoliation methods and applications to photocatalysis: a review

Michelle Saliba,<sup>a</sup> Jean Pierre Atanas,<sup>lb</sup> Tia Maria Howayek<sup>a</sup> and Roland Habchi<sup>ID</sup>\*<sup>ac</sup>

This review provides a deep analysis of the mechanical and optoelectronic characteristics of MoS<sub>2</sub>. It offers a comprehensive assessment of diverse exfoliation methods, encompassing chemical, liquid-phase, mechanical, and microwave-driven techniques. The review also explores MoS<sub>2</sub>'s versatile applications across various domains and meticulously examines its significance as a photocatalyst. Notably, it highlights key factors influencing the photocatalytic process. Indeed, the enhanced visible light responsiveness of materials like MoS<sub>2</sub> holds immense potential across a wide range of applications. MoS<sub>2</sub>'s remarkable photocatalytic response to visible light, coupled with its notable stability, opens up numerous possibilities in various fields. This unique combination makes MoS<sub>2</sub> a promising candidate for applications that require efficient and stable photocatalytic processes, such as environmental remediation, water purification, and energy generation. Its attributes contribute significantly to addressing contemporary challenges and advancing sustainable technologies.

Received 5th September 2023  
Accepted 20th November 2023

DOI: 10.1039/d3na00741c

rsc.li/nanoscale-advances

## 1. Introduction

“The graphene has broken a taboo”, summarizes Vincent Bouchiat following the isolation of graphene in 2004. Since that date, the field of 2D materials has seen the emergence of several new classes of materials that possess unprecedented properties.<sup>1,2</sup>

2D materials, also known as monolayer materials, consist of a single layer of atoms or molecules. Among the most well-known are graphene, molybdenum disulfide (MoS<sub>2</sub>), boron nitride (BN), and phosphorene. These materials possess unique properties that allow them to be used innovatively and versatilely in various applications. These properties, often very different from the same materials at a larger scale, result from quantum confinement and surface effects that occur when bulk materials are reduced to one or a few atomic layers.<sup>1,2</sup>

In fact, the confinement effect is observed when the motion of electrons and holes is restricted in one or more dimensions. This phenomenon, considered a direct consequence of quantum mechanics, manifests itself by the appearance of discrete energy levels and the modification of the bandgap, thereby altering the electronic and optical properties of the material.<sup>4</sup>

Among the 2D materials, transition metal dichalcogenides (TMDCs), often referred to as “the next-generation graphene”,

are gathering increasing interest within the scientific community due to their exceptional properties that cater to a wide range of applications: field-effect transistors (FETs), inverters, photodetectors, light-emitting diodes (LEDs), drug carriers, and bio-detection platforms.<sup>5–10</sup>

Materials in this class have the chemical formula MX<sub>2</sub>, where M represents a transition metal atom (groups 4–12 in the periodic table) and X is a chalcogen (group 16), are called Transition Metal Dichalcogenide (TMDC). They are divided into two categories: metallic TMDCs (MTMDCs) and semi-conducting TMDCs (STMDCs).<sup>2,8,10</sup> In fact, transition metals and chalcogens can form more than 40 types of stable structured transition metal dichalcogenides, each with its characteristics and applications.<sup>8</sup> Some of them are represented in Fig. 1.

Moreover, TMDCs are promising catalytic materials for several applications, including hydrogen production, carbon dioxide reduction, and water purification. Their large specific

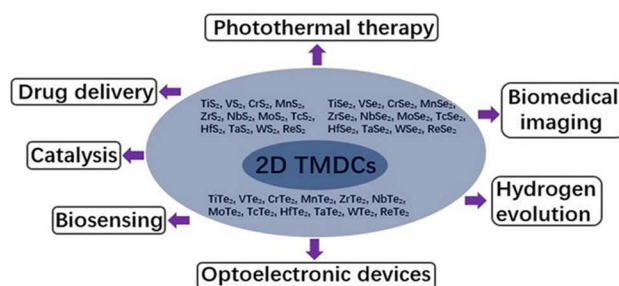


Fig. 1 Different types and applications of TDMCs, adapted from ref. 7 with permission from frontiers copyright 2020.

<sup>a</sup>EC2M, Faculty of Sciences, Fanar, Lebanese University, 2, Campus Pierre Gemayel, 90656, Lebanon. E-mail: rhabchi@ul.edu.lb

<sup>b</sup>University of Balamand Dubai, Department of Physics, D. I. Park-1, Dubai, United Arab Emirates

<sup>c</sup>Functional Materials Group, Gulf University for Science and Technology, Hawally, Kuwait



surface area, high catalytic activity, and capacity to be modified for better performance make them highly attractive catalysts for a variety of chemical reactions.<sup>3,11,12</sup> They also have promising applications in biology due to their ability to interact with biological molecules. They can be used for applications such as biomolecule detection and cellular imaging. In the latter case, TMDCs such as MoS<sub>2</sub> and tungsten sulfide (WS<sub>2</sub>) can be functionalized with antibodies or peptides to target specific proteins within cells. Using fluorescence microscopy, the location of labeled TMDCs can be visualized, allowing for high-resolution imaging.<sup>7,9</sup>

Within this context, TMDCs are an important treatment option in the fight against cancer. Current treatments (chemotherapy and radiotherapy) can be effective, but TMDCs, as drug and diagnostic vectors, offer a potentially more targeted and less invasive alternative. However, more research is needed to develop this method and evaluate its clinical efficacy.<sup>13</sup> Furthermore, TMDCs are an excellent option for Li battery electrodes. Their layered structure allows them to store a large amount of energy, making them highly efficient. Additionally, their ability to be exfoliated into monoatomic layers enables better electrical conductivity, further enhancing their performance as electrodes.<sup>10</sup> On the other hand, when semiconducting TMDCs such as WS<sub>2</sub>, tungsten diselenide (WSe<sub>2</sub>), and MoS<sub>2</sub> are thinned down to a single layer, their electronic structure transitions from an indirect bandgap to a direct bandgap. This modification opens up new applications in the fields of electronics and optoelectronics.<sup>5,6,8,10</sup> MoS<sub>2</sub> and WSe<sub>2</sub> have shown high-quality electronic performances, with high electron mobility, tunable bandgap, strong photoluminescent response, and rapid switching.<sup>8</sup>

Moreover, TMDCs can be modified to form a semiconductor, metal, or superconductor, as well as a material with different magnetic properties, such as ferromagnetic, antiferromagnetic, or paramagnetic.<sup>8</sup>

In summary, TMDCs have the potential to revolutionize numerous technological applications. Their exploitation in all these applications requires a deeper understanding of their physical and chemical properties, as well as continuous improvement of their performances to meet the needs of various applications.<sup>11</sup> Many materials belong to this class, but in this paper, we will focus on the properties and synthesis methods of molybdenum sulfide MoS<sub>2</sub>. This review aims to provide a comprehensive analysis of the synthesis, properties, and various applications of molybdenum oxide, shedding light on its significance in contemporary research and technology. Our primary objective is to explore the diverse range of molybdenum oxide structures and their unique properties, as well as to discuss the latest advancements and emerging trends in its utilization. By synthesizing and evaluating the existing literature, we intend to offer a valuable resource for researchers, scientists, and engineers seeking a deeper understanding of the potential and challenges associated with molybdenum oxide-based materials and their impact on the advancement of technology and sustainable solutions. Through this review, we strive to foster further research and innovation in this promising area of materials science, ultimately contributing to the

development of more efficient and environmentally sustainable technologies.

## 2. Molybdenum sulfide

### 2.1 Structure

Molybdenum disulfide, or molybdenum sulfide (iv), is a blackish-silver solid that occurs in the form of mineral molybdenite, the main molybdenum ore. It is a layered compound that has been used for nearly a century as a solid lubricant and hydroprocessing catalyst.

Monolayers of MoS<sub>2</sub>, like graphene, exhibit a hexagonal atomic lattice in the shape of a honeycomb with a thickness of 0.6 to 0.7 nm. However, they differ in their composition, consisting of three atomic planes instead of one. The Mo plane is sandwiched between two chalcogen planes (S), as illustrated in Fig. 2. Each molybdenum atom (Mo<sup>4+</sup>) is covalently bonded to six sulfur atoms (S<sup>2-</sup>). These anions adopt a trigonal prismatic or octahedral coordination with respect to the metal atoms (see Fig. 3). The layers overlap with each other through van der Waals forces, forming the multilayer material.<sup>2,14</sup>

Furthermore, the stacking of MoS<sub>2</sub> layers gives rise to three main structures, as shown in Fig. 3: trigonal (1T), hexagonal (2H), and rhombohedral (3R), where phase 1T coordinates in an octahedral structure, and 2H and 3R in a trigonal prismatic structure with 1, 2, 3 representing the number of existing layers in each structure. The 1T and 3R structures are metastable, while the 2H structure, the most common in nature, is stable. Additionally, the 1T structure is known to be metallic, while the other two are semiconducting. The lattice constants, properties, and main applications of these structures are summarized in Table 1.<sup>3,15</sup>

Another structure is also found, known as 1T'. It is a less common form that has been discovered recently. It is similar to the 1T structure but with a distortion of the hexagonal lattice, leading to lower symmetry (see Fig. 4). The 1T' phase is more stable than the 1T phase and has a larger bandgap, making it more promising for electronic applications. Research results suggest that the 1T' phase can be synthetically controlled and used for advanced electronic applications.<sup>16</sup>

Moreover, 2D MoS<sub>2</sub> exists in various forms and morphologies, such as nanosheets, nanoflowers, nanoflakes, nanotubes, nanowires, nanoplates, and quantum dots. This variety of forms

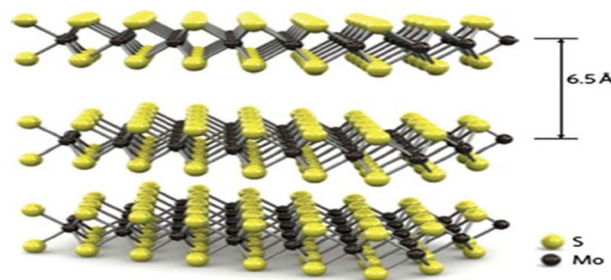


Fig. 2 Crystalline structure of MoS<sub>2</sub>, adapted from ref. 2 from Springer Nature, copyright 2014 (Owned by Springer Nature).



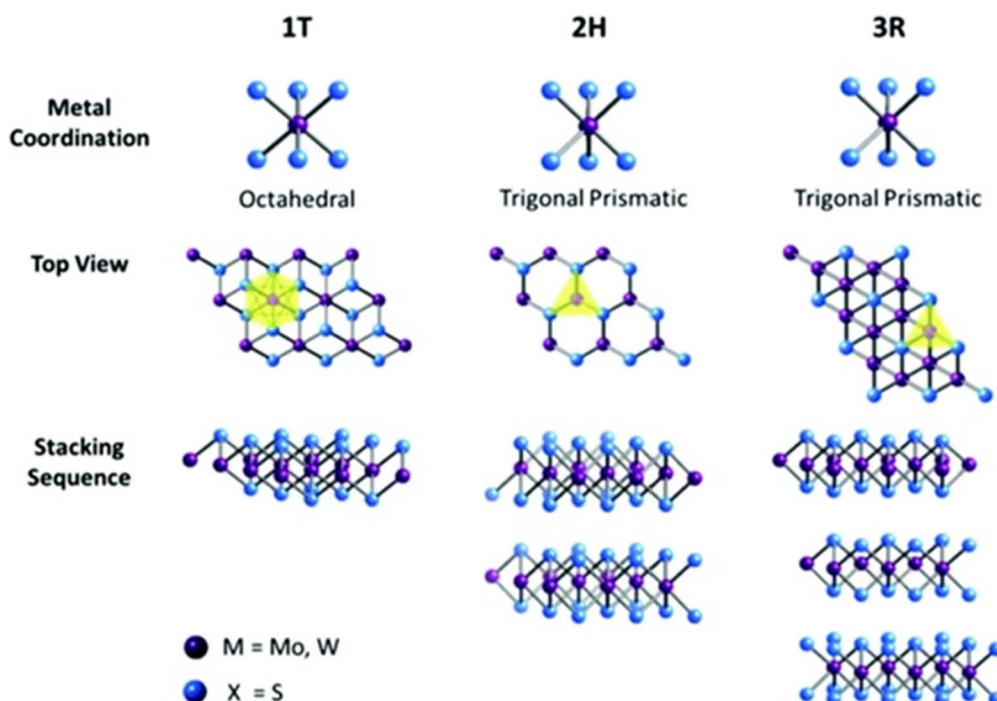


Fig. 3 Different structures and stacking orders of MoS<sub>2</sub> adapted from ref. 3 and 15 with permission from Elsevier, copyright 2021.

can be controlled by choosing appropriate synthesis routes with optimized operational parameters.<sup>17–33</sup>

In fact, when changing the measurement scale, the properties or behavior of materials also change. Thus, individual layers of MoS<sub>2</sub> have radically different properties compared to bulk materials. For example, the surface-to-volume ratio is significantly increased by exfoliation, thereby enhancing the reactivity and catalytic capacity of the materials.<sup>34</sup> Based on this, we will discuss the properties of exfoliated MoS<sub>2</sub>.

## 2.2 Mechanical properties

Molybdenum disulfide (MoS<sub>2</sub>) exhibits exceptional mechanical properties, including high tensile and flexural strength, making it a promising material for sensors, transistors, and flexible electronic devices.<sup>15,35</sup> Additionally, it possesses high wear resistance and low friction, making it an ideal material for

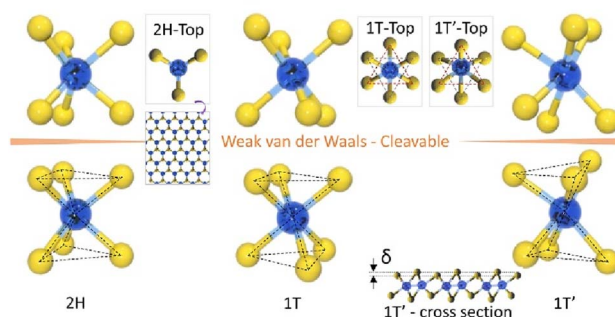


Fig. 4 Typical structures of layered transition metal dichalcogenides. Cleavable 2H, 1T and 1T' structures in layered TMDC, adapted from ref. 6 with permission from Elsevier, copyright 2017.

Table 1 A comparison between the different structures of MoS<sub>2</sub>, adapted from ref. 15 with permission from MDPI, copyright 2021

	1T	2H	3R
Structure coordination	Octahedral	Trigonal prismatic	Trigonal prismatic
Lattice parameters	$a = 5.60 \text{ \AA}$ , $c = 5.99 \text{ \AA}$ and an edge sharing octahedral <sup>34</sup>	$a = 3.15 \text{ \AA}$ , $c = 1230 \text{ \AA}$ <sup>34</sup>	$a = 3.17 \text{ \AA}$ , $c = 18.38 \text{ \AA}$ <sup>34</sup>
Property	Paramagnetic and metallic	Semiconducting	
Electrical conductivity	$10^5$ times higher than 2H phase	Low ( $\sim 0.1 \text{ S m}^{-1}$ )	
Absorption peaks	No peaks at 604 nm and 667 nm	Showed peaks at 604 nm and 667 nm	
Common applications	Intercalation in chemistry	Dry lubricants	Dry lubricants and non-linear optical devices



lubrication applications.<sup>15</sup> However, the impact of defects on these properties has been studied using computer simulations. These studies have revealed that the presence of randomly dispersed defects in the monolayer of MoS<sub>2</sub> can significantly reduce its elastic constants, which may alter its mechanical performance.<sup>35</sup> Bertolazzi and his team<sup>36</sup> conducted experiments to measure the stiffness and rupture strength of a monolayer of MoS<sub>2</sub> using an atomic force microscope tip on a pre-patterned silicon dioxide (SiO<sub>2</sub>) substrate. The results showed an effective Young's modulus of 270 ± 100 GPa and an average rupture strength of 23 GPa. Similarly, Castellanos-Gomez and colleagues<sup>37</sup> studied the mechanical properties of suspended MoS<sub>2</sub> nanosheets, ranging from 5 to 25 layers, and obtained an average Young's modulus of 330 ± 70 GPa. These experiments clearly demonstrated that 2D MoS<sub>2</sub> is an extremely strong material capable of withstanding large elastic deformations. However, the study conducted by Rahman and his team revealed that high-temperature oxidation causes significant changes in the structure and mechanical properties of MoS<sub>2</sub>. The results showed notable deterioration in mechanical properties such as rupture strength, rupture strain, Young's modulus, and toughness. Oxidation leads to the breaking of chemical bonds between molybdenum and sulfur atoms, thereby weakening the material's mechanical strength.<sup>38</sup>

Recently, Sun *et al.* performed in-depth DFT calculations to evaluate the mechanical properties of six elements from the TMDC family (MoS<sub>2</sub>, MoSe<sub>2</sub>, niobium disulfide (NbS<sub>2</sub>), niobium diselenide (NbSe<sub>2</sub>), rhenium disulfide (ReS<sub>2</sub>), rhenium diselenide (ReSe<sub>2</sub>)). They reported that, although these materials exhibit relatively low Young's modulus, shear modulus, and tensile strength compared to graphene, they are more robust for structural in-plane deformations and more resistant to buckling. Additionally, some of them have higher rupture strains than graphene, which is the case for MoS<sub>2</sub>, where the strain can even exceed 0.4 in uniaxial tension.<sup>39</sup> Furthermore, it has been shown that monolayer or few-layer MoS<sub>2</sub> has a stiffness comparable to steel, and both functionalized and non-functionalized MoS<sub>2</sub> nanosheets can act as reinforcement additives for different types of polymer matrices such as polystyrene (PS), polyvinyl acetate (PVA), and thermoplastic polyurethane (TPU).<sup>19,40</sup> In this context, Ahmadi *et al.* demonstrated that a small amount of functionalized MoS<sub>2</sub> nanosheets (0.5% by weight) is sufficient to improve the mechanical properties of PS, PVA, and TPU, including tensile strength and Young's modulus.<sup>19</sup>

### 2.3 Opto-electronic properties

Molybdenum disulfide (MoS<sub>2</sub>) is a two-dimensional material that exhibits fascinating opto-electronic properties. These properties are influenced by various factors, such as its band structure, number of layers, nanostructure size, doping, applied strain, and the presence of defects and impurities.<sup>41–44</sup> By understanding these factors, it becomes possible to optimize the opto-electronic properties of MoS<sub>2</sub> for specific applications.

MoS<sub>2</sub> is a semiconductor with a direct band gap of approximately 1.8 eV in a single layer and an indirect band gap of about 1.2 eV starting from two layers. The direct band gap is located at the *K* point in the Brillouin zone, while the indirect band gap has its peak at the *Γ* point and its minimum between *Γ* and *K* (see Fig. 5). As the number of MoS<sub>2</sub> layers decreases, the energy of the conduction band minimum increases due to quantum confinement, leading to a transition from an indirect to a direct band gap. This transition from near-infrared to visible range opens up numerous possibilities for applications while altering the optical and electronic properties of the material.<sup>4,42,43</sup>

Photoluminescence is a phenomenon in which MoS<sub>2</sub> emits light after absorbing energy. The photoluminescence properties of MoS<sub>2</sub> are influenced by factors such as the material's thickness, temperature, and interactions with the environment.<sup>45</sup> A study conducted by Wang *et al.* demonstrated that electron injection can enhance photoluminescence and cause a spectral shift in a single layer of MoS<sub>2</sub>. These enhancements have significant implications in the field of opto-electronic applications. A more intense photoluminescence can be advantageous for light-emitting devices like MoS<sub>2</sub>-based light-emitting diodes (LEDs). Additionally, the spectral shift can be utilized to adjust the range of wavelengths emitted by MoS<sub>2</sub>, which is beneficial for detection and optical communication applications.<sup>46</sup> The mobility of charge carriers in MoS<sub>2</sub> is a crucial parameter for evaluating its performance as a semiconductor. The electronic mobility of MoS<sub>2</sub> has been extensively studied, and values have been reported in the literature. At room temperature, the electron mobility of MoS<sub>2</sub> has been measured to be around 410 cm<sup>2</sup> V<sup>-1</sup> s<sup>-1</sup>, which is lower than the theoretical limit and has not yet reached competitive levels compared to silicon. However, ongoing research aims to improve the charge carrier mobility in MoS<sub>2</sub> using different techniques and strategies, such as growing high-quality films, employing high-permittivity dielectric materials, and introducing dopants. These efforts seek to increase the

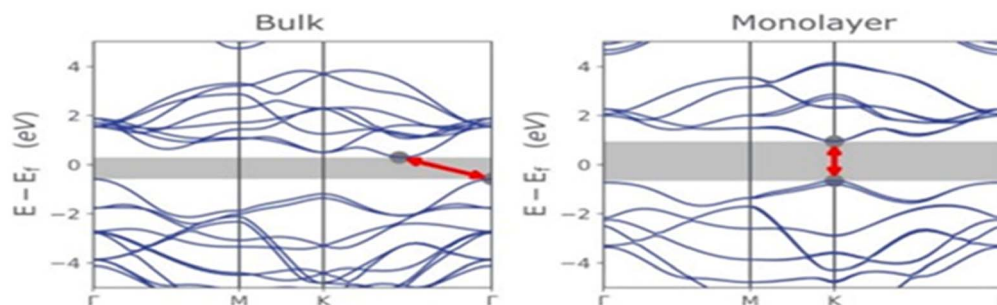


Fig. 5 Energy band structure diagrams of bulk and monolayer MoS<sub>2</sub>. Adapted from ref. 4 with permission from MDPI, copyright 2022.



electron mobility of MoS<sub>2</sub> and open up new possibilities for its applications in electronic and opto-electronic devices.<sup>47</sup> MoS<sub>2</sub> holds great potential for a wide range of opto-electronic applications, including light-emitting diodes, solar cells, optical sensors, phototransistors, lasers, and optical modulators. Its unique properties, combined with flexibility, transparency, and compatibility with flexible substrates, make it a promising material for flexible electronics and integrated opto-electronic devices.<sup>48–52</sup> Furthermore, by combining MoS<sub>2</sub> with other materials, such as surface plasmons, its optical properties can be modulated for advanced applications, such as controlled light emission and ultrafast opto-electronic devices.<sup>53</sup>

## 2.4 Harnessing MoS<sub>2</sub> for environmental and energy solutions

Molybdenum disulfide (MoS<sub>2</sub>), a versatile and potent photocatalyst, holds exceptional promise in addressing critical environmental and energy challenges. Its practical prospects are manifold, with a focus on sustainability, clean energy generation, and environmental remediation.

**2.4.1 Environmental remediation.** MoS<sub>2</sub> plays a pivotal role in the cleanup of environmental pollutants. Its high charge transfer properties and reactive surface make it a formidable tool in the degradation of a wide array of contaminants. From vibrant dyes to persistent pesticides and complex pharmaceutical compounds, MoS<sub>2</sub> has demonstrated remarkable efficacy in reducing these pollutants to harmless byproducts. This not only helps restore environmental balance but also contributes to the protection of ecosystems and public health.

**2.4.2 Clean energy generation.** The role of MoS<sub>2</sub> in clean energy generation cannot be overstated. Its utility in the efficient conversion of sunlight into chemical energy positions it as a key player in the realm of renewable energy. MoS<sub>2</sub>-based photocatalytic systems hold the potential to harness solar energy for hydrogen production from water. This not only offers a sustainable source of hydrogen, a clean fuel, but also mitigates the environmental impact associated with traditional fossil fuel combustion.

**2.4.3 Carbon emission mitigation.** One of the most urgent global challenges is the reduction of carbon emissions. MoS<sub>2</sub> contributes significantly to this endeavor by catalyzing the conversion of carbon dioxide (CO<sub>2</sub>) into valuable chemicals, including hydrocarbons and alcohols. This transformative process not only mitigates CO<sub>2</sub> levels in the atmosphere but also upcycles this greenhouse gas into valuable raw materials, reducing the carbon footprint of industries.

**2.4.4 Synergistic composites for enhanced efficiency.** Innovative combinations of MoS<sub>2</sub> with other materials, such as semiconductor nanocomposites, have shown promise in achieving unprecedented levels of photocatalytic efficiency. This synergy brings forth new horizons in sustainable technology, providing practical solutions for complex energy and environmental issues. The development of such composite materials enhances the efficiency and performance of photocatalytic reactions, making them increasingly applicable in real-world settings.

**2.4.5 Challenges and the path forward.** While MoS<sub>2</sub> has made significant strides in addressing environmental and energy challenges, there remain areas for improvement. Optimizing visible light absorption, managing active catalytic sites, and enhancing the durability of MoS<sub>2</sub>-based photocatalysts are key challenges. To fully harness the practical prospects of MoS<sub>2</sub> in addressing these challenges, ongoing research and innovation are essential. As scientists and engineers continue to refine its properties and applications, MoS<sub>2</sub> stands as a beacon of hope for a cleaner, more sustainable future.

In conclusion, MoS<sub>2</sub>'s potential to address environmental and energy challenges is not just theoretical; it is deeply rooted in its remarkable properties and demonstrated capabilities. With continued research, development, and integration into practical solutions, MoS<sub>2</sub> has the potential to be a driving force in the transition to a more sustainable and environmentally friendly world.

## 3. Synthesis methods of molybdenum disulfide

The synthesis of MoS<sub>2</sub> at the nanoscale has attracted increasing research and investment due to its potential applications in catalysis, electrochemistry, and opto-electronics. In fact, the weak van der Waals forces between MoS<sub>2</sub> layers have led to various synthesis techniques, each resulting in different quantities, shapes, and sizes of products. These techniques can be classified into two categories: (i) the top-down method, where the properties of a sample evolve from a macroscopic size to a nanometric dimension, and (ii) the bottom-up method, which assembles MoS<sub>2</sub> nanosheets using individual atoms.<sup>2,3</sup> Each of these methods has its advantages and disadvantages and can be used based on specific needs for MoS<sub>2</sub> synthesis.<sup>54</sup> Exfoliation is one of the top-down techniques characterized by low controllability and relatively high cost. It involves separating MoS<sub>2</sub> layers from each other to obtain mono or a few-layered MoS<sub>2</sub> sheets. However, achieving controlled synthesis of such fascinating materials is a crucial issue. In this section, we will summarize the different types of exfoliations commonly adopted, including chemical exfoliation, liquid-phase exfoliation, mechanical exfoliation and microwave-driven exfoliation.

### 3.1 Chemical exfoliation

Chemical exfoliation, sometimes considered a solvent-based exfoliation method, can be divided into two types: intercalation exfoliation and electrochemical exfoliation. The method of chemical exfoliation of MoS<sub>2</sub> through intercalation involves separating the material's layers through chemical reactions. This method is the oldest and most popular for the scalable synthesis of MoS<sub>2</sub>. It allows the production of high-quality MoS<sub>2</sub> nanoflakes in large quantities.<sup>55</sup> This technique involves the insertion of ions into the interlayer space between MoS<sub>2</sub> layers. When the ions are inserted, they create an expansion force that forces the molybdenum disulfide layers to separate. This separation can be aided by applying mechanical force or gentle agitation.<sup>55</sup> Researchers often use ultrasonication for this



purpose. The use of ultrasonication coupled with intercalation can help produce atomically thin MoS<sub>2</sub> layers more rapidly and efficiently while improving the quality of the samples produced. It has been demonstrated that this method can significantly reduce the lateral size of nanoflakes<sup>17,56</sup> and can lead to sufficiently small monolayer MoS<sub>2</sub> quantum dots (QDs) after repeated exfoliation.<sup>57</sup> However, this method requires significant expertise and faces challenges for large-scale production. Studies have shown that increasing the input power and using a higher ultrasound frequency can improve the quality and thickness of nanoflakes.<sup>58,59</sup> However, prolonged sonication may cause defects in the structures, reducing its effectiveness in industrial applications, particularly in circuits and other electronic devices.<sup>56</sup> Ultrasonication generates pressure waves that can facilitate intercalating compounds to infiltrate more easily between sulfur layers. The addition of ultrasound can, therefore, reduce the time required for intercalation. Additionally, during mechanical exfoliation, ultrasound can help separate MoS<sub>2</sub> layers by acting on the adhesive forces between them, reducing the intensity of mechanical force required for exfoliation, thus reducing the risk of damaging the thin layers produced.<sup>58</sup> After intercalation, the atomically thin MoS<sub>2</sub> layers can be isolated using transfer methods such as filtration or deposition onto a substrate. The properties of the resulting thin layers depend on the homogeneous realization of intercalation, the size and shape of the MoS<sub>2</sub> foundations, the properties of the intercalating compounds, the application method, and the exfoliation conditions. Characterization techniques such as transmission electron microscopy, Raman spectroscopy, and photoluminescence can be used to characterize the structural, electronic, and optical properties of the resulting layers.

Indeed, intercalation can be performed with various ions, such as lithium, potassium, sodium, ammonium, phosphorus, chlorine, *etc.* The choice of the intercalating ion depends on several factors, such as the size and polarizability of the ion, the intercalation rate, the stability of the obtained MoS<sub>2</sub> nanoflakes, the ease of recovering the intercalating ion, *etc.* Yang *et al.* used sodium ions (Na<sup>+</sup>) as an intercalation agent to facilitate the exfoliation of MoS<sub>2</sub> nanoflakes. By combining liquid-phase reflux assisted by Na<sup>+</sup> and ultrasound treatment in *N*-methyl-2-pyrrolidone (NMP) solvent, they successfully obtained fine and uniform MoS<sub>2</sub> nanoflakes. Moreover, these exfoliated nanoflakes showed improved properties, particularly in the field of photocatalytic applications.<sup>61</sup> However, the most commonly used intercalating ion is lithium (Li<sup>+</sup>). The small size of lithium ions allows them to intercalate reversibly into lamellar-structured materials while filling the vacant interstitial sites.<sup>62</sup> When bulk crystals are placed in a solution acting as a source of lithium ions (usually *n*-butyllithium dissolved in hexane), these ions diffuse between the MoS<sub>2</sub> layers and distribute unevenly among the layers, leading to locally high Li content with high reducibility. This high content of lithium produces defects in MoS<sub>2</sub>, making it more fragile. Following ultrasonication, the layers separate, resulting in the formation of a monolayer or a few-layer MoS<sub>2</sub>.<sup>57,62</sup> The resulting layers tend to have the metallic 1T structure, which is less desirable than the semiconductor 2H structure. However, the 1T structure can

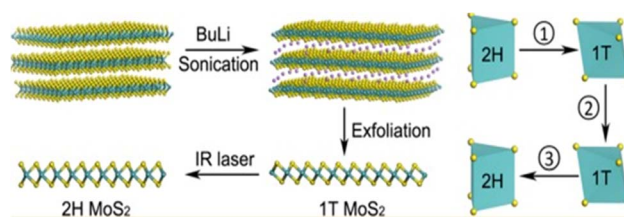


Fig. 6 Schematic description of the main mechanisms of exfoliation by intercalation. Adapted from ref. 17 (*Nano Lett.*, 2015, 15(9), 5956–5960), copyright (2015), American Chemical Society.

be converted to 2H through thermal annealing.<sup>17,18,62</sup> All these steps are simplified in Fig. 6.

Exfoliation through intercalation with Li is an effective method for producing layers of MoS<sub>2</sub> with remarkable mechanical and electrical properties, such as high-performance field-effect transistors and highly efficient solar cells. It can also enhance the photocatalytic activity of MoS<sub>2</sub> under visible light.<sup>54</sup> Additionally, the use of different organolithium compounds, such as methyl-lithium (Me-Li), butyl-lithium (*n*-Bu-Li), and *tert*-butyllithium (*t*-Bu-Li), can result in varying degrees of exfoliation, which impacts the electrochemical properties of MoS<sub>2</sub> as well as its capacitive and catalytic properties for the hydrogen evolution reaction.<sup>63</sup> However, this method requires meticulous control of experimental parameters to achieve a high yield of monolayers.

Recently, electrochemistry has been considered as an alternative method for producing two-dimensional materials in a liquid medium. Electrochemical exfoliation of layered materials takes place in an electrolytic cell where a fixed potential is applied between the layered crystal and a counter electrode, both immersed in an electrolyte that facilitates the intercalation of ionic species between the layers. Ionic intercalation weakens the interlayer forces in the bulk crystal, while the coulombic repulsion between charged layers and the formation of gas molecules lead to the exfoliation of the material (see Fig. 7(c)).<sup>64</sup> Electrochemical exfoliation has been highly successful because, unlike other liquid exfoliation approaches, it allows for the production of significant quantities of MoS<sub>2</sub> nanosheets on the order of grams per hour, which can be collected in powder form. The produced material is remarkably rich in monolayers and bilayers, with lateral sizes in the micrometer range. Additionally, the production process is extremely fast, taking only a few minutes to a few hours, depending on the desired material quantity. Moreover, it requires mild conditions and very basic equipment. Electrochemical exfoliation can take place in an aqueous solution without the use of harmful reagents or aggressive reaction conditions. Therefore, the key advantage of electrochemical exfoliation lies in its high efficiency.<sup>64</sup> The device commonly used for electrochemical exfoliation is a simple electrolytic cell, consisting of two electrodes, an electrolyte, and a power source. The working electrode is the material to be exfoliated, and the counter electrode is typically a platinum wire as a less expensive option. Electrochemical exfoliation can occur under either anodic or cathodic conditions, depending on the electrolyte and applied potential. This



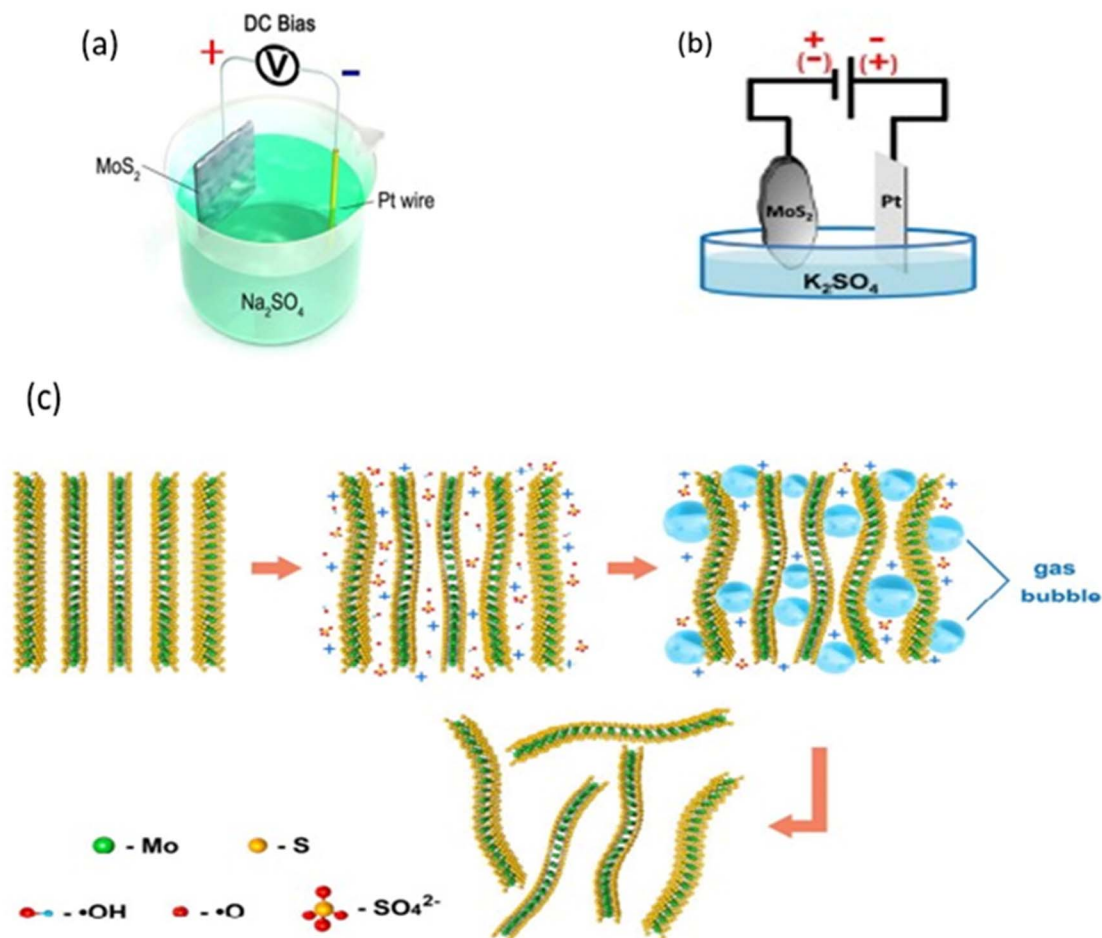


Fig. 7 (a) Schematic illustration of the experimental setup for the anodic electrochemical exfoliation of bulk MoS<sub>2</sub> crystal. (b) Schematic diagram of the electrochemical setup for exfoliation of natural MoS<sub>2</sub> crystals. (c) Schematic illustration of the electrochemical exfoliation mechanism. Adapted with permission from ref. 65 (*ACS Nano*, 2014, 8(7), 6902–6910) Copyright (2014) American Chemical Society.

means that the working electrode can be positively or negatively charged, allowing for the intercalation of either anions or cations, respectively.<sup>64</sup>

Anodic exfoliation occurs by applying a positive voltage to the working electrode, leading to the intercalation of negative ions present in the solution into the layered crystal. This exfoliation is commonly performed in an aqueous solution.<sup>64</sup> In 2014, Liu *et al.* proposed a mechanism for the anodic exfoliation of MoS<sub>2</sub> in an aqueous solution of sodium sulfate Na<sub>2</sub>SO<sub>4</sub>. When a positive voltage is applied, the oxidation of water or sulfate ions SO<sub>4</sub><sup>2-</sup> results in the formation of hydroxyl radicals OH· and oxide radicals O·. These radicals insert themselves between the layers of MoS<sub>2</sub>, significantly increasing the inter-layer spacing. During this oxidation process, gases such as oxygen (O<sub>2</sub>) and/or sulfur dioxide (SO<sub>2</sub>) are produced, further contributing to the expansion of the spacing and, consequently, the exfoliation of the material. However, it is important to note that the electro-oxidation reaction primarily occurs at the surface of the bulk material's electrode, leading to rapid oxidation of the formed products. This rapid oxidation may impact the quality and degree of exfoliation of MoS<sub>2</sub>. Additionally, the nanoflakes obtained by this method are

characterized by considerably larger size (5–50 μm) compared to those obtained by other exfoliation methods (see Fig. 7(a)).<sup>65</sup> By applying a negative voltage, it is possible to drive the intercalation of positive ions in the solution into a layered crystal used as the cathode in an electrolytic cell. Cathodic exfoliation is typically performed in organic solvents such as dimethyl sulfoxide (DMSO).<sup>18–64</sup> El Garah *et al.* presented a rapid (<1 hour) electrochemical exfoliation method for molybdenum disulfide (MoS<sub>2</sub>) using lithium-ion intercalation, with a lithium chloride solution in DMSO as the electrolyte. Their results pave the way for a rapid and ambient condition preparation of MoS<sub>2</sub> nanoflakes with an average lateral size of about 0.8 μm, suitable for low-cost electronic (optoelectronic) devices. Their intercalation/exfoliation approach enables the preparation of predominantly semiconducting nanoflakes, with a phase 2H content of approximately 60%, unlike previous chemical or electrochemical methods that resulted in metallic nanoflakes with a phase 1T content exceeding 60%. The transition from the 2H phase to the 1T phase during intercalation is usually attributed to a significant transfer of electrons from lithium atoms to the MoS<sub>2</sub> layers. However, in this case, the presence of DMSO molecules coordinating the Li ions could attenuate the



intercalation step and thus limit the electron transfer process, preventing the conversion to the metallic 1T phase.<sup>18</sup> Zhang *et al.* successfully achieved efficient exfoliation of natural MoS<sub>2</sub> crystal using an electrochemical method. Their approach led to the production of large MoS<sub>2</sub> flakes, reaching sizes of up to 50 μm, with a high yield of approximately 70%. To carry out this electrochemical exfoliation, an experimental setup was employed, consisting of a piece of MoS<sub>2</sub> crystal as the working electrode, a platinum (Pt) foil as the counter electrode, and tetra-*n*-butylammonium bisulfate (TBA·HSO<sub>4</sub>) as the electrolyte. Since the tetra-*n*-butylammonium cations (TBA<sup>+</sup>) are larger than the spacing between the MoS<sub>2</sub> layers, a positive voltage of +5 V was applied for 5 minutes to intercalate SO<sub>4</sub><sup>2-</sup> anions, thereby expanding the crystal and allowing for the corresponding cation intercalation. Subsequently, a negative voltage of −5 V was applied to initiate exfoliation, resulting in the formation of gas bubbles and the dissociation of the MoS<sub>2</sub> crystal into small pieces in the electrolyte.<sup>66</sup> Anodic and cathodic exfoliation can be performed simultaneously in some cases during electrochemical exfoliation. This can be done for various reasons, such as maximizing exfoliation, improving the quality of the obtained nanoflakes, controlling the size of the nanoflakes, *etc.* In this context, Ambrosi and Pumera offered a reliable alternative to the Li intercalation/exfoliation approach, not only for catalytic applications like hydrogen evolution reaction but also for other applications where the semiconductor 2H properties are preferred. They used a natural MoS<sub>2</sub> crystal as the working electrode and a platinum electrode as the counter electrode. By applying alternative anodic and cathodic voltages, they succeeded in generating the release of fine MoS<sub>2</sub> nanoflakes in the solution (Fig. 7(b)). This method significantly increased the active surface area of MoS<sub>2</sub>, favoring the electrogeneration of hydrogen.<sup>12</sup>

In summary, chemical exfoliation through intercalation and electrochemical exfoliation are effective methods for producing MoS<sub>2</sub> nanoflakes with remarkable mechanical and electrical properties. These methods are crucial for various applications, including high-performance field-effect transistors, high-efficiency solar cells, and improved photocatalytic activity under visible light.

### 3.2 Liquid phase exfoliation

Liquid phase exfoliation (LPE) of molybdenum disulfide (MoS<sub>2</sub>) involves dissolving MoS<sub>2</sub> crystals in a solvent or solution and then exfoliating them into thin layers using mechanical, chemical, or thermal techniques. This method is widely used because it is simple, cost-effective, and efficient for producing MoS<sub>2</sub> sheets with exceptional properties.<sup>64</sup> Liquid phase exfoliation of MoS<sub>2</sub> offers other advantages, such as control over the thickness of exfoliated flakes, ease of chemical modification of flake surfaces, and the versatility of support materials, making it widely used in the production of various applications, such as electronic devices, sensors, and catalysts.<sup>64</sup> Several solvents are used to achieve MoS<sub>2</sub> exfoliation, including water, alkaline solutions (such as sodium carbonate Na<sub>2</sub>CO<sub>3</sub> or potassium hydroxide KOH), and organic solvents (such as *N*-

methylpyrrolidone NMP, dimethylformamide DMF, acetone, and chloroform). Using water as a solvent for exfoliation has certain advantages. According to a recent study, water can be used as an alternative to organic solvents for dispersing MoS<sub>2</sub> nanoflakes.<sup>67</sup> Although water dispersions are not as stable as those in organic solvents, the obtained nanoflakes can have lateral dimensions ranging from 500 nm to 50 μm and are stabilized by electric charges.<sup>68</sup> Furthermore, Gupta *et al.* showed that an appropriate amount of water added to NMP not only significantly improves exfoliation yields and stabilizes the nanoflakes for a long time but also reduces the defect densities of exfoliated nanoflakes.<sup>69</sup> However, water is not traditionally considered a good solvent for exfoliating two-dimensional (2D) materials due to surface energy disparities.<sup>70</sup> Its use for MoS<sub>2</sub> exfoliation may be limited because MoS<sub>2</sub> can have a strong affinity with water and may re-agglomerate, limiting the quality of the exfoliation achieved. Additionally, alkaline solutions have potential advantages for MoS<sub>2</sub> exfoliation, including efficient and environmentally friendly synthesis, as well as the production of smaller nanoflakes than the bulk material. Wu *et al.* developed a cost-effective and sustainable method for producing MoS<sub>2</sub> nanoflakes using a mixed alkaline solution of lithium hydroxide/sodium hydroxide (LiOH/NaOH). The resulting nanoflakes exhibited improved anti-friction and anti-wear properties when used as a lubricating additive. The technique proved to be more effective than other methods, and the thickness and lateral size of the prepared MoS<sub>2</sub> nanoflakes were reduced, showing nanoflakes with approximately 2 to 9 layers.<sup>71</sup> Organic solvents play a crucial role in the exfoliation process. The selection of solvents depends on several parameters such as surface tension and Hildebrand and Hansen solubility parameters. The Hildebrand parameter refers to a numerical estimation of the degree of interaction between materials, indicating miscibility, and Hansen parameters evaluate three characteristics of molecules: dispersion forces, intermolecular forces, and hydrogen bonding, to predict the possibility of mutual dissolution of materials and the formation of a solution.<sup>72,73</sup> Exfoliation has been found to be highly effective when the solvent's surface tension matches well with that of MoS<sub>2</sub>.<sup>72</sup> In fact, to achieve high-quality liquid phase exfoliation and large-scale synthesis, it is imperative to minimize the change in Gibbs free energy ( $\Delta G$ ) during exfoliation. Surface tension is caused by intermolecular attraction between the solid surface and solvent droplet, and the difference in surface tension results in a change in Gibbs free energy during exfoliation. For efficient LPE and large-scale synthesis, it is essential to minimize the Gibbs free energy change ( $\Delta G$ ).<sup>22</sup> However, it is essential to note that each material has specific solvent requirements for effective exfoliation.<sup>74</sup>

Among organic solvents, *N*-methylpyrrolidone (NMP) is the most commonly used solvent for MoS<sub>2</sub> exfoliation, especially for applications related to sensors and electronics. It can provide stable dispersion of MoS<sub>2</sub> flakes with controlled thickness and long shelf life. However, NMP has disadvantages, including high cost, toxicity, negative environmental impact, and high evaporation temperature. Therefore, exploring other polar solvents for MoS<sub>2</sub> exfoliation is important.<sup>14,22,54</sup> Sahoo *et al.*





presented a cost-effective chemical method to synthesize MoS<sub>2</sub> nanoflakes using acetone as a solvent. Various concentrations (0.08–0.4 mg ml<sup>-1</sup>) of samples were prepared by mixing crushed and dried MoS<sub>2</sub> powder with 30 ml of acetone. The suspension was then subjected to high-intensity sonication for up to 30 hours. The method resulted in the production of nanoflakes with approximately 2 to 7 layers, exhibiting efficient photocatalytic performance in decomposing methylene blue dye. Additionally, the authors<sup>22</sup> found that the response to visible light of MoS<sub>2</sub> nanoflakes strongly depended on the number of layers. In particular, MoS<sub>2</sub> nanoflakes prepared from an initial bulk concentration of 0.08 mg ml<sup>-1</sup> showed the maximum degradation compared to other samples.<sup>22</sup> Muscuso *et al.* studied the exfoliation behavior of MoS<sub>2</sub> in isopropyl alcohol (IPA) using intensive sonication. They found that the IPA solvent improved the exfoliation process, resulting in thin flakes and small lateral particle sizes within a narrow range (1.5–6 nm). However, the dispersion was not stable for long periods due to re-stacking and sedimentation phenomena.<sup>75</sup>

### 3.3 Mechanical exfoliation

At the end of the 19th century, Spring and Lea were pioneers in conducting systematic investigations in the field of mechanochemistry. Although its development was slow, mechanochemistry saw a decisive turning point in the 1960s with the emergence of methodological advancements, notably the invention of mechanical alloying.<sup>76</sup> In 2004, researchers A. K. Geim and K. S. Novoselov successfully isolated graphene using a micromechanical exfoliation method.<sup>77</sup> This technique, commonly known as the “Scotch-tape” method, involves repeated cleavages of the material using adhesive tape to obtain a single layer or a few layers of the material. It is a relatively simple method to implement, producing high-quality materials with minimal defects and crystal sizes ranging from the nanoscale to several micrometers. However, the yield of this process is very low.<sup>78</sup>

While mechanical exfoliation using adhesive tape was the first successful method for isolating 2D materials, ball milling utilizes a similar technique but is more suitable for large-scale production. Initially used to fragment and mix metallic powders to manufacture alloys, ball milling is now used for large-scale exfoliation of 2D materials in layers. As the balls roll and rebound in the mill with the 2D material, they apply shear, rolling, and impact forces, breaking van der Waals bonds and separating the 2D layers.<sup>64</sup> This technique can generally be classified into two categories: dry ball milling and wet ball milling. The latter requires the use of a special and expensive organic solvent, which can lead to pollution and high costs.<sup>24,78</sup> However, dry ball milling is very aggressive and can cause defects in the basal plane and on the edges of the layered materials.<sup>78</sup> These defects, in reality, are beneficial for modifying the properties of 2D materials in applications such as energy storage. They offer additional active adsorption sites, promote faster diffusion, and increase storage capacity.<sup>79</sup> Determining the milling parameters is essential to ensure the quality and yield of the product. Among these parameters are

the milling intensity, milling atmosphere, ratio of ball mass to powder mass, and the ratio of the occupied volume to the free volume of the jar.<sup>64</sup> In their research, Tayebbi *et al.*<sup>80</sup> systematically studied the operating parameters of ball milling in the exfoliation of bulk MoS<sub>2</sub> using sodium cholate (SC) as an exfoliant. They monitored the yield and dimensions of exfoliated MoS<sub>2</sub> nanoflakes by modifying parameters such as the weight ratio between bulk MoS<sub>2</sub> and SC (SC/MoS<sub>2</sub>), jar filling rate, ball size (dB), mill rotation speed (nR), and initial mass of bulk MoS<sub>2</sub> (mMoS<sub>2</sub>). Under the following optimal conditions, SC/MoS<sub>2</sub> = 0.75, 50% filling rate, and mMoS<sub>2</sub> = 0.20 g, they reported a high yield of 95% of exfoliated nanoflakes.<sup>80</sup>

Recently, aqueous-phase mechanical exfoliation has presented several advantages such as immediate functionalization, controllable size, environmentally friendly and scalable operation. Deng *et al.* developed a two-step strategy to produce high-quality ultrathin 2D nanoflakes, with a thickness of about 1 nm. The first step involved using ball milling to mechanically insert alkali metal atoms (lithium (Li), sodium (Na), or potassium (K)) into the layered materials, forming metal intercalation compounds. In the second step, these compounds were dissolved in pure water at 60 °C, resulting in a violent reaction generating hydrogen (H<sub>2</sub>) and alkali metal hydroxide, which caused exfoliation. They also demonstrated that this method enabled the production of a series of amorphous 2D nanomaterials with heterostructures composed of two or more components and multiple interfaces, with a yield of up to 97.5%.<sup>20</sup> Liu and Kumatsu proposed a simple and effective alternative to produce MoS<sub>2</sub> and WS<sub>2</sub> nanoflakes using sodium cholate as a surfactant during the milling process to facilitate exfoliation and dispersion of the nanoflakes in water. They showed that the exfoliated sample can be stored as a “solid stock” and easily dispersed in water by manual agitation, resulting in highly concentrated dispersions of MoS<sub>2</sub> and WS<sub>2</sub> nanoflakes with yields reaching 93% and 57%, respectively, after centrifugation.<sup>21</sup> The innovative approach of hydrothermal-assisted ball milling has sparked considerable interest due to its promising potential for commercial applications. In a recent study, Ahmadi *et al.*<sup>19</sup> presented a method combining hydrothermal autoclave and ball milling to produce high-quality functionalized MoS<sub>2</sub> nanoflakes for polymer nanocomposites on a large scale. The production process involves using an acetone solution containing diaminodiphenyl sulfone (DDS) to prepare MoS<sub>2</sub> precursors, followed by intercalation and exfoliation in the hydrothermal autoclave to form MoS<sub>2</sub> powders intercalated with DDS. These powders are then subjected to ball milling, resulting in MoS<sub>2</sub> nanoflakes. The obtained nanoflakes had an average lateral dimension greater than 640 nm, with a thickness of about 6 nm and a high specific surface area of 121.8 m<sup>2</sup> g<sup>-1</sup>.<sup>19</sup>

### 3.4 Microwave-driven exfoliation

Microwave-driven exfoliation has introduced a groundbreaking technique for the efficient production of MoS<sub>2</sub> nanosheets. By utilizing the distinctive heating characteristics of microwave radiation, this novel approach facilitates the controlled



exfoliation of individual layers from bulk MoS<sub>2</sub> source materials. The method takes advantage of the interaction between electromagnetic waves and the polar molecules within the material, leading to rapid localized heating. This phenomenon initiates thermal stress and expansion within the material, resulting in the separation of MoS<sub>2</sub> layers. One of the key advantages of this process is its ability to significantly reduce processing time and energy consumption when compared to traditional exfoliation methods.<sup>81</sup> This advancement has the potential to transform the field of MoS<sub>2</sub> production and open new avenues for its utilization in various applications. The technique involves a series of intricate steps to achieve successful exfoliation. Initially, the bulk MoS<sub>2</sub> material is meticulously prepared, which can take the form of powders or solid pieces. To ensure optimal exfoliation, the bulk material is dispersed within a suitable solvent. This solvent not only aids in the dispersion of MoS<sub>2</sub> layers but also prevents their re-aggregation throughout the exfoliation process. As a result, stable nanosheets are formed. The dispersion is subsequently exposed to controlled microwave irradiation. The unique ability of microwaves to penetrate materials and interact with polar molecules leads to rapid and even heating within the dispersion. This induces thermal expansion and mechanical stress between the layers of MoS<sub>2</sub>, prompting their separation into individual nanosheets. The process can be observed in real-time as the material heats up, affording precise control over the desired thickness of the nanosheets. This innovative technique holds promise for efficient and controlled production of MoS<sub>2</sub> nanosheets with potential implications across various applications. The effectiveness of this approach is heavily dependent on the careful optimization of various process parameters. Among these, the selection of the solvent is of paramount importance, as it significantly influences both the extent of exfoliation and the overall quality of the produced nanosheets. Likewise, meticulous calibration of the microwave power and duration of irradiation is essential. These parameters must be finely tuned to ensure uniform and reliable exfoliation without inducing any undesirable material degradation. Striking the right balance among these factors is crucial for generating MoS<sub>2</sub> nanosheets of exceptional quality and tailored characteristics.<sup>81</sup> The resulting nanosheets exhibit unique electronic, optical, and mechanical properties that make them exceptionally promising for a wide range of applications across electronics, optoelectronics, energy storage, and more.<sup>82–84</sup> To exemplify this potential, a study by Mohammad-Andashti *et al.* showcased the versatility of MoS<sub>2</sub> quantum dots, synthesized through microwave-driven exfoliation. These quantum dots served as a versatile platform for fluorescence-based biosensing applications, particularly in the detection of cortisol levels in human saliva.<sup>84</sup> Advanced microscopy techniques, such as Atomic Force Microscopy (AFM) and Transmission Electron Microscopy (TEM), play a pivotal role in the meticulous examination of various aspects of the nanosheets, including layer count, dimensions, and structural characteristics. This comprehensive characterization not only provides valuable insights into the uniformity and quality of the exfoliated nanosheets but also contributes to the optimization of the exfoliation process.<sup>81,82</sup>

The microwave-driven exfoliation represents an innovative and promising method for the controlled production of MoS<sub>2</sub> nanosheets. By harnessing the unique heating properties of microwave radiation to induce controlled thermal stress and expansion, this technique offers a rapid, efficient, and potentially scalable pathway to obtaining high-quality nanosheets with customized properties.

In resume, determining the “best” method for exfoliating molybdenum oxide depends on the specific application and desired material properties. Each exfoliation method has its advantages and limitations, and the choice of method should align with the intended use of the exfoliated molybdenum oxide. Here's a brief overview of each method:

**Chemical exfoliation:** this method involves the use of chemical agents to break down the bulk molybdenum oxide into layered or single-layer sheets. It can be effective in achieving a high degree of exfoliation but may require the use of potentially hazardous chemicals. The choice of chemicals and reaction conditions can influence the quality and yield of the exfoliated material.

**Liquid phase exfoliation:** liquid phase exfoliation typically employs solvents to disperse and exfoliate molybdenum oxide. It is a scalable and versatile method that allows for the production of stable dispersions. The choice of solvent and sonication conditions can impact the quality of the exfoliated sheets.

**Mechanical exfoliation:** this method involves physically cleaving bulk molybdenum oxide using techniques like scotch tape or mechanical shear. It is straightforward but less scalable. Mechanical exfoliation is useful for producing high-quality single-layer materials but may not be practical for large-scale production.

**Microwave-driven exfoliation:** microwave-assisted exfoliation is a relatively new method that uses microwave radiation to exfoliate materials. It can be efficient in producing exfoliated molybdenum oxide sheets and has the potential for industrial scale-up.

The choice of the “best” method depends on factors such as the desired quality of the exfoliated material, scalability, safety, and the specific application. For example, if you require a small quantity of high-quality single-layer molybdenum oxide for fundamental research, mechanical or liquid phase exfoliation might be preferred. On the other hand, if you need a larger quantity for an industrial application, microwave-driven or chemical exfoliation might be more suitable. Ultimately, the selection of the best method should be based on a careful evaluation of the specific requirements of your research or application.

Below is Table 2 in which a comparison of the exfoliation methods is presented.

## 4. Photocatalysis

### 4.1 Principle of catalysis

Catalysis is a fundamental phenomenon that modifies the kinetics and outcomes of chemical reactions in the presence of a catalyst. The catalyst acts by reducing the activation energy

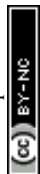


Table 2 A comparison list between different exfoliation methods

Exfoliation method	Quality of exfoliation	Scalability	Safety concerns	Application suitability
Chemical exfoliation	High-quality sheets	May be scalable with proper equipment	Potential safety concerns due to chemical use	Versatile, suitable for various applications
Liquid phase exfoliation	Good quality, stable dispersions	Scalable, ideal for larger quantities	Safer than chemical methods	Suitable for applications requiring dispersions
Mechanical exfoliation	High-quality single-layer sheets	Less scalable, labor-intensive	Relatively safe	Ideal for fundamental research, small quantities
Microwave-driven exfoliation	Potential for high-quality exfoliation	May be scalable with proper equipment	Safety concerns related to microwave use	Promising for industrial applications, fast exfoliation

required for the reaction, thereby accelerating the conversion of reactants into products. An essential characteristic of catalysis is that the catalyst itself is not consumed or chemically altered during the process, allowing for its recovery and subsequent reuse.<sup>85</sup> There are two types of catalysis: homogeneous catalysis, where the catalyst and reactants are in the same phase.<sup>85</sup> Heterogeneous catalysis, where the catalyst, usually in solid form, is in a different phase from the reactants (gas or liquid). In this case, the reaction occurs on the surface of the catalyst. The process involves the adsorption of reactants on the catalyst's surface, the actual chemical reaction, and the desorption of products from the catalyst's surface.<sup>85</sup>

#### 4.2 Photocatalysis mechanism

Photocatalysis represents a particular catalytic process sensitive to both light and a photocatalyst. It involves utilizing appropriate light to activate a photocatalyst, thus altering the rate of a chemical reaction without depleting the photocatalyst itself. To put it concisely, photocatalysis is a chemical reaction occurring in the presence of a photocatalyst and suitable light. In essence, this reaction forces light to generate excited electrons and positive holes, initiating redox reactions as its initial step, encompassing both positive and negative Gibbs-energy changes. An effective photocatalyst typically takes the form of a conductive nanomaterial capable of absorbing incident light, elevating itself to higher energy states, which, in turn, imparts this energy to a reacting substance, facilitating a chemical reaction. Particularly when applied to energy-demanding processes like photosynthesis, photocatalysis holds great promise as a sustainable solution for large-scale solar energy production, conversion, and storage. Moreover, photocatalysis offers significant potential in the realm of environmental remediation.<sup>86</sup>

In semiconductors, the photocatalysis relies on the excitation by a light radiation whose energy corresponds to the width of its bandgap. The determination of this energy is based on the equation  $\lambda = hc/E$ , where  $h$  and  $c$  represent the Planck constant and the speed of light, respectively. For example, TiO<sub>2</sub> (anatase) has a bandgap of  $\sim 3.2$  eV, which means it can only be excited by ultraviolet photons with a wavelength less than approximately 390 nm. On the other hand, bulk MoS<sub>2</sub> has a smaller bandgap of 1.3 eV, allowing it to capture a larger part of the solar spectrum. As the number of MoS<sub>2</sub> layers decreases, the bandgap gradually

increases, reaching 1.9 eV for a monolayer, enabling it to use visible light with a wavelength less than 660 nm.<sup>34</sup> When the catalyst is exposed to an appropriate light source, photons with sufficient energy are absorbed, leading to the generation of electron-hole pairs. These pairs are essential for establishing a redox system, allowing for: the capture of electrons by acceptors such as oxygen (O<sub>2</sub>), leading to the formation of oxygen radicals such as superoxides (O<sub>2</sub><sup>•-</sup>) and hydroperoxyl radicals (HO<sub>2</sub><sup>•</sup>). The filling of holes by electron donors, such as organic pollutants, which can be directly oxidized or give rise to hydroxyl radicals (OH<sup>-</sup>) from adsorbed species like water (H<sub>2</sub>O). These generated radicals (Fig. 8) enable the degradation of a wide range of pollutants, including volatile organic compounds and pharmaceutical products.

In the absence of appropriate electron acceptors and donors, electron/hole recombination occurs (a very rapid recombination reaction on the order of picoseconds). Electron/hole recombination is a limiting factor in the efficiency of this method, as the probability of recombination is approximately 99.9%. There are several solutions to increase photocatalytic efficiency, such as doping the semiconductor with other metals (to extend the absorption range to the visible spectrum) or adding electron acceptors to the reaction medium (ozone, hydrogen peroxide, ferric ions Fe<sup>3+</sup>, *etc.*) to limit charge recombination.

#### 4.3 Key parameters of photocatalysis

The efficiency of photocatalytic reactions depends on various parameters. In this context, we can mention the concentration

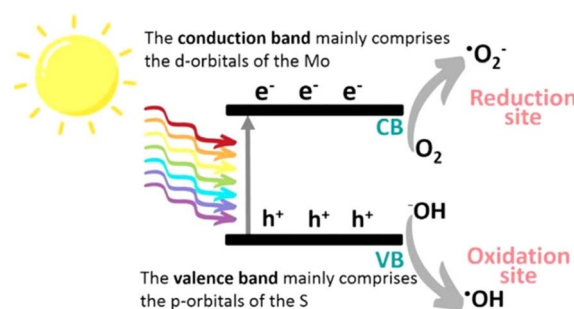


Fig. 8 Schematic illustration of the photocatalytic mechanism of MoS<sub>2</sub>.<sup>94</sup> Adapted with permission from (*ACS Omega*, 2022, 7(26), 22089–22110). Copyright (2022) American Chemical Society.



and surface state (charge, adsorbed species, defects, composition) of the catalyst, the conditions of the reaction environment (temperature, pressure, pH, solvent, ...), the concentration and adsorption of reactants, the oxygen concentration, and the light source (wavelength, intensity, distance).<sup>87–90</sup> Some of the key parameters include:

**Photon flux.** For the photocatalytic reaction to occur, a light source (UV or visible) must irradiate the catalyst's surface to excite it. Therefore, the degradation rate increases with the photon flux. However, once a certain value is reached, which varies depending on the specific system studied, the degradation rate remains constant even if the flux continues to increase. It is crucial not to exceed this limit of photon flux to avoid wasting energy unnecessarily.

**Catalyst mass.** The reaction rate increases proportionally with the quantity of catalyst until it reaches a plateau where it remains constant. It is even possible that the reaction rate decreases at high catalyst concentrations. This decrease in reaction rate is attributed to the screening effect of particles that prevent light from reaching the surface of a part of the catalyst.

**Initial concentration of reactants.** The reaction rate is dependent on the initial concentration of the reactant ( $C_0$ ) and follows the Langmuir–Hinshelwood mechanism.<sup>91</sup> At low concentration, the reaction rate is proportional to the reactant concentration. When all active sites of the photocatalyst are saturated, the reaction rate becomes independent of the concentration.

**Dissolved oxygen.** Oxygen is a reactant that plays a crucial role in forming  $O_2^{\cdot-}$  species, which prevents the recombination of electron–hole pairs. Therefore, it is necessary to have a significant concentration of dissolved oxygen to promote the degradation kinetics of organic compounds. The oxygen level is usually ensured by simple air supply rather than injecting pure oxygen (for economic reasons).

**Operating conditions.** The adsorption of reactants on the surface of the photocatalyst is a spontaneous and exothermic process that is closely related to temperature. At low temperatures, the amount of available thermal energy is reduced, favoring the adsorption of reactants on the photocatalyst's surface. It is worth noting that this adsorption can also involve the final products, which may act as inhibitors. However, at high temperatures, thermal agitation increases, favoring desorption reactions and leading to the detachment of products from the photocatalyst's surface. Therefore, it is essential to maintain the temperature within an optimal range, typically between 20 °C and 80 °C, to optimize the reaction efficiency.

Moreover, pH plays a significant role in the kinetics of photocatalytic reactions. Depending on the pH value, the catalyst surface can become charged, affecting its interactions with molecules in the solution. The semiconductor has a point of zero charge (PZC), where its surface is neutral. If the pH is lower than the PZC pH, the surface will be positively charged, while if the pH is higher, it will be negatively charged. Additionally, depending on the pKa of the considered molecule, it may take a charged or uncharged form depending on the pH value of the medium. Thus, the interactions between the material and

molecules may vary depending on the pH, impacting the reaction kinetics.

#### 4.4 Photocatalytic applications of MoS<sub>2</sub>

**4.4.1 Chalcogenides as promising photocatalysts.** Chalcogenides, a class of semiconductors, have emerged as prominent materials in the realm of photocatalysis due to their remarkable properties, most notably their narrow band gap energy. This attribute is of particular significance in the context of visible light-induced photocatalysis, where the ability to harness the energy of visible light for chemical reactions holds immense promise. Chalcogenides can be categorized into several types, including binary, multinary, and chalcogenide-based heterostructures, each of which exhibits unique and intricate photocatalytic mechanisms. One of the primary challenges in photocatalysis is the rapid recombination of photogenerated electron–hole pairs, and chalcogenides offer opportunities for addressing this issue through various strategies.<sup>95</sup>

**4.4.2 MoS<sub>2</sub> as a versatile photocatalyst.** Among the myriad chalcogenides, molybdenum disulfide (MoS<sub>2</sub>) has garnered considerable attention as a highly promising photocatalyst. Recent studies have delved into diverse applications of MoS<sub>2</sub> in the realm of photocatalysis, capitalizing on its exceptional charge transfer properties and reactive surface. For instance, MoS<sub>2</sub> has been employed with great success in the degradation of a range of organic pollutants, encompassing dyes, pesticides, and pharmaceutical compounds.<sup>3,92–94</sup> This efficacy is attributed to MoS<sub>2</sub>'s ability to facilitate charge separation and reduce electron–hole recombination, thereby enhancing the photocatalytic performance.

**4.4.3 Synergistic enhancements through composites.** Innovative approaches involve combining MoS<sub>2</sub> with other materials, such as semiconductor nanocomposites, to create synergistic systems. By coupling MoS<sub>2</sub> with complementary materials, researchers have achieved significant improvements in photocatalytic efficiency. This synergy often arises from the cooperative interaction between MoS<sub>2</sub> and the partner materials, leading to enhanced catalytic performance.<sup>23,96–99</sup>

**4.4.4 Hydrogen production and CO<sub>2</sub> reduction.** MoS<sub>2</sub> exhibits great promise in the realm of hydrogen production from water. Recent studies have demonstrated its utility as a cocatalyst in combination with other photocatalytic materials, resulting in improved hydrogen production activity. Moreover, the tunability of MoS<sub>2</sub>'s morphology and particle size has been explored to fine-tune the efficiency and stability of photocatalytic reactions.<sup>98,99</sup>

In the context of CO<sub>2</sub> reduction, MoS<sub>2</sub> plays a vital role in catalyzing the conversion of carbon dioxide into valuable chemicals, including hydrocarbons and alcohols. This catalytic activity stems from MoS<sub>2</sub>'s exceptional electron transfer properties, which enhance its performance as an active site for CO<sub>2</sub> reduction reactions.<sup>100</sup>

**4.4.5 Remaining challenges and future prospects.** Despite the impressive strides in harnessing MoS<sub>2</sub> for photocatalysis, several challenges remain to be addressed. These include improving visible light absorption, optimizing active catalytic



sites, and enhancing the overall durability of MoS<sub>2</sub>-based photocatalysts. Continued research and development efforts are essential to unlock the full potential of MoS<sub>2</sub> and further advance its role as an efficient and long-lasting photocatalyst in diverse applications.

## 5. Conclusion

Molybdenum disulfide (MoS<sub>2</sub>) is an exceptional two-dimensional material with remarkable properties such as high electrical and thermal conductivity, increased mechanical strength, notable chemical stability, and considerable specific surface area. These intrinsic characteristics give this material strong potential for various applications, including solar cells, sensors, batteries, catalysts, and electronics. Two-dimensional MoS<sub>2</sub>-based materials have garnered significant interest due to their proven potential in addressing environmental issues and their ability to meet the growing demand for energy. Their exceptional ability to absorb visible light opens promising perspectives for harnessing solar energy, an abundant and economically advantageous energy source. Additionally, the transition of MoS<sub>2</sub> from the third to the second dimension induces significant modifications in its band structure, characterized by the widening of the bandgap, thereby conferring improved optoelectronic properties to the material. It is also worth noting that the number of layers present in the material directly impacts its physical and chemical properties. In particular, MoS<sub>2</sub> nanoflakes in a single layer have demonstrated superior photocatalytic activity compared to those with multiple layers. These features make MoS<sub>2</sub> a promising photocatalyst for environmental and energy-related applications. Furthermore, the different crystalline phases observed in MoS<sub>2</sub> play a crucial role in its electronic properties and band structure. Therefore, a thorough understanding and mastery of these different phases are essential to optimize the performance of two-dimensional MoS<sub>2</sub>-based materials in various applications. Various strategies are implemented for the synthesis of reduced-dimension MoS<sub>2</sub>, including liquid exfoliation, chemical exfoliation, and mechanical exfoliation. The latter offers the advantage of a high yield of MoS<sub>2</sub> nanoflakes, although they may be thicker and less regular. This method requires specialized equipment but has the economic advantage of limiting the use of chemicals. In contrast, liquid and chemical exfoliation allows better control over the dimensions, morphology, and orientation of nanoflakes, although it may entail higher costs due to the use of solvents or chemical reagents. Additionally, the quantity produced may be limited depending on the solubility or chemical reactivity of the material. The choice of the method will depend on the specific needs of the application, considering the inherent advantages and disadvantages of each approach.

In summary, despite the challenges related to the preparation of two-dimensional MoS<sub>2</sub>, its distinctive properties and versatility generate significant interest in the fields of research and development. Continuous improvement of synthesis methods and in-depth understanding of its characteristics will enable the optimal exploitation of the potential of two-

dimensional MoS<sub>2</sub>, fostering innovative and sustainable applications.

As for future research directions for MoS<sub>2</sub> in photocatalysis, we should aim to further unlock the potential of MoS<sub>2</sub> and address key challenges. As an example, efforts should be directed toward enhancing the visible light absorption of MoS<sub>2</sub>-based photocatalysts. Strategies may include bandgap engineering, surface modification, and heterostructure formation to expand the spectrum of light that can be utilized for photocatalytic reactions.<sup>101,102</sup>

Controlling and optimizing the distribution of active catalytic sites on MoS<sub>2</sub> surfaces is also essential. Future research should explore innovative methods for precise site engineering, which can improve catalytic efficiency and selectivity while minimizing energy losses.<sup>103,104</sup>

Further investigations into the controlled synthesis of MoS<sub>2</sub> with specific morphologies and particle sizes are crucial. This can lead to improved photocatalytic performance by optimizing the exposed surface area and electronic properties of MoS<sub>2</sub>.<sup>105,106</sup>

Furthermore, exploring the integration of MoS<sub>2</sub> into photovoltaic devices is a growing field. Research should focus on utilizing MoS<sub>2</sub> in solar cells to enhance energy conversion efficiency, and further studies on charge separation and electron transport are warranted.<sup>107,108</sup>

The use of MoS<sub>2</sub> for environmental remediation should be expanded. Future research can investigate the degradation of emerging contaminants and industrial effluents, and explore the scalability and practicality of MoS<sub>2</sub>-based photocatalytic systems for water treatment.<sup>109,110</sup>

The potential of MoS<sub>2</sub> in synergy with other nanomaterials, such as graphene, metal oxides, or carbon nanotubes, is a fertile area for exploration. These composite systems can offer enhanced photocatalytic performance and may open doors to novel applications.<sup>111,112</sup>

## Conflicts of interest

There are no conflicts to declare.

## Acknowledgements

Dr Habchi would like to thank the scientific research support program of the Lebanese University.

## References

- 1 V. Shanmugam, R. Mensah, K. Babu, S. Gawusu, A. Chanda, Y. Tu, R. Neisiany, M. Försth, G. Sas and O. Das, A review of the synthesis, properties, and applications of 2D materials, *Part. Part. Syst. Charact.*, 2022, **39**(6), 2200031.
- 2 A. B. Kaul, Two-dimensional layered materials: Structure, properties, and prospects for device applications, *J. Mater. Res.*, 2014, **29**(3), 348–361.
- 3 N. Thomas, S. Mathew, K. M. Nair, K. O'Dowd, P. Forouzandeh, A. Goswami, G. McGranaghan and S. C. Pillai, 2D MoS<sub>2</sub>: structure, mechanisms, and



- photocatalytic applications, *Mater. Today Sustain.*, 2021, **13**, 100073.
- 4 L. Ali, F. Subhan, M. Ayaz, S. ul Hassan, C. Byeon, J. Kim and S. Bungau, Exfoliation of MoS<sub>2</sub> Quantum Dots: Recent Progress and Challenges, *Nanomaterials*, 2022, **12**(19), 3465.
  - 5 T. Tan, X. Jiang, C. Wang, B. Yao and H. Zhan, 2D material optoelectronics for information functional device applications: status and challenges, *Advanced Science*, 2020, **7**(11), 2000058.
  - 6 W. Choi, N. Choudhary, G. H. Han, J. Park, D. Akinwande and Y. H. Lee, Recent development of two-dimensional transition metal dichalcogenides and their applications, *Mater. Today*, 2017, **20**(3), 116–130.
  - 7 X. Zhou, H. Sun and X. Bai, Two-dimensional transition metal dichalcogenides: synthesis, biomedical applications and biosafety evaluation, *Front. Bioeng. Biotechnol.*, 2020, **8**, 236.
  - 8 M. Wu, Y. Xiao, Y. Zeng, Y. Zhou, X. Zeng, L. Zhang and W. Liao, Synthesis of two-dimensional transition metal dichalcogenides for electronics and optoelectronics, *InfoMat*, 2021, **3**(4), 362–396.
  - 9 A. K. Mia, M. Meyyappan and P. K. Giri, Two-dimensional transition metal dichalcogenide based biosensors: from fundamentals to healthcare applications, *Biosensors*, 2023, **13**(2), 169.
  - 10 L. Song, H. Li, Y. Zhang and J. Shi, Recent progress of two-dimensional metallic transition metal dichalcogenides: Syntheses, physical properties, and applications, *J. Appl. Phys.*, 2022, **131**(6), 060902.
  - 11 L. Lei, D. Huang, G. Zeng, M. Cheng, D. Jiang, C. Zhou, S. Chen and W. Wang, A fantastic two-dimensional MoS<sub>2</sub> material based on the inert basal planes activation: Electronic structure, synthesis strategies, catalytic active sites, catalytic and electronics properties, *Coord. Chem. Rev.*, 2019, **399**, 213020.
  - 12 A. Ambrosi and M. Pumera, Electrochemical exfoliation of MoS<sub>2</sub> crystal for hydrogen electrogeneration, *Chem.-Eur. J.*, 2018, **24**(69), 18551–18555.
  - 13 M. J. Molaei, Two-dimensional (2D) materials beyond graphene in cancer drug delivery, photothermal and photodynamic therapy, recent advances and challenges ahead: A review, *J. Drug Delivery Sci. Technol.*, 2021, **61**, 101830.
  - 14 X. Li and H. Zhu, Two-dimensional MoS<sub>2</sub>: Properties, preparation, and applications, *J. Mater.*, 2015, **1**(1), 33–44.
  - 15 O. Samy, Sh. Zeng, M. D. Birowosuto and A. El Moutaouakil, A review on MoS<sub>2</sub> properties, synthesis, sensing applications and challenges, *Crystals*, 2021, **11**(4), 355.
  - 16 A. K. Singha, P. Kumar, D. J. Late, A. Kumar, S. Patel and J. Singh, 2D layered transition metal dichalcogenides (MoS<sub>2</sub>): synthesis, applications and theoretical aspects, *Appl. Mater. Today*, 2018, **13**, 242–270.
  - 17 X. Fan, P. Xu, D. Zhou, Y. Sun, Y. C. Li, M. Nguyen, M. Terrones and T. E. Mallouk, Fast and Efficient Preparation of Exfoliated 2H-MoS<sub>2</sub> Nanosheets by Sonication-Assisted Lithium Intercalation and Infrared Laser-Induced 1T to 2H Phase Reversion, *Nano Lett.*, 2015, **15**, 5956–5960.
  - 18 M. El Garah, S. Bertolazzi, S. Ippolito, M. Eredia, I. Janica, G. Melinte, O. Ersen, G. Marletta, A. Ciesielski and P. Samori, MoS<sub>2</sub> nanosheets *via* electrochemical lithium-ion intercalation under ambient conditions, *FlatChem.*, 2018, **9**, 33–39.
  - 19 M. Ahmadi, O. Zabihi, Q. Li, S. M. Fakhrhoseini and M. Naebe, A Hydrothermal-Assisted Ball Milling Approach for Scalable Production of High-Quality Functionalized MoS<sub>2</sub> Nanosheets for Polymer Nanocomposites, *Nanomaterials*, 2019, **9**, 1400.
  - 20 C. Deng, Y. Gao, Y. Yao, B. Liang, S. Lu and T. Tao, Conversion of layered materials to ultrathin amorphous nanosheets induced by ball-milling insertion and pure-water exfoliation, *J. Mater. Chem. A*, 2022, **10**, 11766.
  - 21 G. Liu and N. Komatsu, Readily Available “Stock Solid” of MoS<sub>2</sub> and WS<sub>2</sub> Nanosheets through Solid-Phase Exfoliation for Highly Concentrated Dispersions in Water, *ChemNanoMet*, 2016, **2**, 500–503.
  - 22 D. Sahoo, B. Kumar, J. Sinha, S. Ghosh, S. S. Roy and B. Kaviraj, Cost effective liquid phase exfoliation of MoS<sub>2</sub> nanosheets and photocatalytic activity for wastewater treatment enforced by visible light, *Sci. Rep.*, 2020, **10**, 10759.
  - 23 W. Liu, Q. Hu, F. Mo, J. Hu, Y. Feng, H. Tang, H. Ye and S. Miao, Photo-catalytic degradation of methyl orange under visible light by MoS<sub>2</sub> nanosheets produced by H<sub>2</sub>SiO<sub>3</sub> exfoliation, *J. Mol. Catal. A: Chem.*, 2014, **395**, 322–328.
  - 24 J. Huang, Y. Liu, P. Yan, J. Gao, Y. Fan and W. Jiang, Mechanically exfoliated MoS<sub>2</sub> nanoflakes for optimizing the thermoelectric performance of SrTiO<sub>3</sub>-based ceramic composites, *J. Mater.*, 2022, **8**(4), 790–798.
  - 25 D. Shi, M. Yang, B. Chang, Z. Ai, K. Zhang, Y. Shao, Sh. Wang, Y. Wu and X. Hao, Ultrasonic-Ball Milling: A Novel Strategy to Prepare Large-Size Ultrathin 2D Materials, *Small*, 2020, **16**(13), 1906734.
  - 26 J. Wu, M. Lin, L. Wang and T. Zhang, Photoluminescence of MoS<sub>2</sub> prepared by effective grinding-assisted sonication exfoliation, *J. Nanomater.*, 2014, **2014**, 107.
  - 27 A. Gupta, V. Arunachalam and S. Vasudevan, Liquid-phase exfoliation of MoS<sub>2</sub> nanosheets: the critical role of trace water, *J. Phys. Chem. Lett.*, 2016, **7**(23), 4884–4890.
  - 28 S. Priya, D. Mandal, A. Chowdhury, S. Kansala and A. Chandra, Time-dependent exfoliation study of MoS<sub>2</sub> for its use as a cathode material in high-performance hybrid supercapacitors, *Nanoscale Adv.*, 2023, **5**(4), 1172–1182.
  - 29 S. Kim, W. Park, D. Kim, J. Kang, J. Lee, H. Y. Jang, S. H. Song, B. Cho and D. Lee, Novel exfoliation of high-quality 2H-MoS<sub>2</sub> nanoflakes for solution-processed photodetector, *Nanomaterials*, 2020, **10**(6), 1045.
  - 30 P. Chithaiah, S. Ghosh, A. Idelevich, L. Rovinsky, T. Livneh and A. ZaK, Solving the “MoS<sub>2</sub> nanotubes” synthetic enigma and elucidating the route for their catalyst-free and scalable production, *ACS Nano*, 2020, **14**(3), 3004–3016.



- 31 Y. Jiaa, Y. Maa, Y. Lina, J. Tanga and W. Shia, Facile synthesis of branched MoS<sub>2</sub> nanowires, *Chem. Phys.*, 2018, **513**, 209–212.
- 32 F. Arshad, C. Aubry, F. Ravaux and L. Zou, 2D MoS<sub>2</sub> nanoplatelets for fouling resistant membrane surface, *J. Colloid Interface Sci.*, 2021, **590**, 415–423.
- 33 A. Thomas and K. B. Jinesh, Excitons and Trions in MoS<sub>2</sub> Quantum Dots: The Influence of the Dispersing Medium, *ACS Omega*, 2022, **7**(8), 6531–6538.
- 34 Z. Wang and B. Mi, Environmental applications of 2D molybdenum disulfide (MoS<sub>2</sub>) nanosheets, *Environ. Sci. Technol.*, 2017, **51**(15), 8229–8244.
- 35 M. J. Akhter, W. Kus, A. Mrozek and T. Burczynski, Mechanical properties of monolayer MoS<sub>2</sub> with randomly distributed defects, *Materials*, 2020, **13**(6), 1307.
- 36 S. Bertolazzi, J. Brivio and A. Kis, Stretching and breaking of ultrathin MoS<sub>2</sub>, *ACS Nano*, 2011, **5**(12), 9703–9709.
- 37 A. Castellanos-Gomez, M. Poot, G. A. Steele, H. S. J. van der Zant, N. Agrait and G. Rubio-Bollinger, Elastic properties of freely suspended MoS<sub>2</sub> nanosheets, *Adv. Mater.*, 2012, **24**(6), 772–775.
- 38 Md. H. Rahman, E. H. Chowdhury and S. Hong, High temperature oxidation of monolayer MoS<sub>2</sub> and its effect on mechanical properties: A ReaxFF molecular dynamics study, *Surf. Interfaces*, 2021, **26**, 101371.
- 39 H. Sun, P. Agrawala and C. V. Singh, A first-principles study of the relationship between modulus and ideal strength of single-layer, transition metal dichalcogenides, *Mater. Adv.*, 2021, **2**(20), 6631–6640.
- 40 M. B. Khan, R. Jan, A. Habib and A. N. Khan, Evaluating mechanical properties of few layers MoS<sub>2</sub> nanosheets-polymer composites, *Adv. Mater. Sci. Eng.*, 2017, 2017.
- 41 D. P. Rai, T. V. Vu, A. Laref, M. P. Ghimire, P. K. Patra and S. Srivastava, Electronic and optical properties of 2D monolayer (ML) MoS<sub>2</sub> with vacancy defect at S sites, *Nano-Struct. Nano-Objects*, 2020, **21**, 100404.
- 42 B. Zhua, J. Langa and Y. H. Hua, S-Vacancy induced indirect-to-direct band gap transition in multilayer MoS<sub>2</sub>, *Phys. Chem. Chem. Phys.*, 2020, **22**(44), 26005–26014.
- 43 A. Taffelli, S. Dirè, A. Quaranta and L. Pancheri, MoS<sub>2</sub> based photodetectors: a review, *Sensors*, 2021, **21**(8), 2758.
- 44 B. Song, H. Gu, M. Fang, Y. Ho, X. Chen, H. Jiang and Sh. Liu, Complex optical conductivity of two-dimensional MoS<sub>2</sub>: A striking layer dependency, *J. Phys. Chem. Lett.*, 2019, **10**(20), 6246–6252.
- 45 S. Golovynskya, I. Irfana, M. Bosib, L. Seravallib, O. I. Datsenkoc, I. Golovynskaa, B. Lia, D. Lina and J. Qu, Exciton and trion in few-layer MoS<sub>2</sub>: Thickness-and temperature-dependent photoluminescence, *Appl. Surf. Sci.*, 2020, **515**, 146033.
- 46 J. Wang, Z. Han, Z. He, K. Wang, X. Liu and A. V. Sokolov, Tip-enhanced photoluminescence of monolayer MoS<sub>2</sub> increased and spectrally shifted by injection of electrons, *Nanophotonics*, 2023, 2937–2943.
- 47 Sh. H. Mir, V. K. Yadav and J. K. Singh, Recent advances in the carrier mobility of two-dimensional materials: a theoretical perspective, *ACS Omega*, 2020, **5**(24), 14203–14211.
- 48 C. Lattyak, M. Vehse, M. A. Gonzalez, D. Pareek, L. Gütay, S. Schäfer and C. Agert, Optoelectronic Properties of MoS<sub>2</sub> in Proximity to Carrier Selective Metal Oxides, *Adv. Opt. Mater.*, 2022, **10**(9), 2102226.
- 49 O. A. Abbas, C. Huang, D. W. Hewak, S. Mailis and P. Sazio, Opto-electronic properties of solution-synthesized MoS<sub>2</sub> metal-semiconductor-metal photodetector, *Opt. Mater.: X*, 2022, **13**, 100135.
- 50 S. García-Dalí, J. I. Paredes, J. M. Munuera, S. Villar-Rodil, A. Adawy, A. Martínez-Alonso and J. M. D. Tascón, Aqueous cathodic exfoliation strategy toward solution-processable and phase-preserved MoS<sub>2</sub> nanosheets for energy storage and catalytic applications, *ACS Appl. Mater. Interfaces*, 2019, **11**(40), 36991–37003.
- 51 Y. Zhang, X. Chen, H. Zhang, Sh. Hu, G. Zhao, M. Zhang, W. Qin, Z. Wang, X. Huang and J. Wang, Facile Exfoliation for High-Quality Molybdenum Disulfide Nanoflakes and Relevant Field-Effect Transistors Developed With Thermal Treatment, *Front. Chem.*, 2021, **9**, 650901.
- 52 M. T. L. Lai, K. M. Lee, T. C. K. Yang, G. T. Pan, C. W. Lai, C. Chen, M. R. Johana and J. C. Juan, The improved photocatalytic activity of highly expanded MoS<sub>2</sub> under visible light emitting diodes, *Nanoscale Adv.*, 2021, **3**(4), 1106–1120.
- 53 A. Zada, P. Muhammad, W. Ahmad, Z. Hussain, Sh. Ali, M. Khan, Q. Khan and M. Maqbool, Surface plasmonic-assisted photocatalysis and optoelectronic devices with noble metal nanocrystals: design, synthesis, and applications, *Adv. Funct. Mater.*, 2020, **30**(7), 1906744.
- 54 J. Sun, X. Li, W. Guo, M. Zhao, X. Fan, Y. Dong, C. Xu, J. Deng and Y. Fu, Synthesis methods of two-dimensional MoS<sub>2</sub>: A brief review, *Crystals*, 2017, **7**(7), 198.
- 55 D. Pariari and D. D. Sarmaa, Nature and origin of unusual properties in chemically exfoliated 2D MoS<sub>2</sub>, *APL Mater.*, 2020, **8**, 4.
- 56 Z. Xiao, C. H. Xie, Y. Wang, R. Chen and Sh. Wang, Recent advances in defect electrocatalysts: Preparation and characterization, *J. Energy Chem.*, 2021, **53**, 208–225.
- 57 W. Qiaoa, Sh. Yana, X. Songa, X. Zhanga, X. Hea, W. Zhonga and Y. Du, Luminescent monolayer MoS<sub>2</sub> quantum dots produced by multi-exfoliation based on lithium intercalation, *Appl. Surf. Sci.*, 2015, **359**, 130–136.
- 58 D. Y. Hoo, Z. L. Low, D. Y. S. Low, S. Y. Tang, S. Manickam, K. Wei Tan and Z. Hong Ban, Ultrasonic cavitation: An effective cleaner and greener intensification technology in the extraction and surface modification of nanocellulose, *Ultrason. Sonochem.*, 2022, 106176.
- 59 M. Telkhozhayeva, E. Teblum, R. Konar, O. Girshevitz, I. Perelshstein, H. Aviv, Y. R. Tischler and G. D. Nessim, Higher ultrasonic frequency liquid phase exfoliation leads to larger and monolayer to few-layer flakes of 2D layered materials, *Langmuir*, 2021, **37**(15), 4504–4514.
- 60 W. Qiao, Sh. Yan, X. He, X. Song, Z. Li, X. Zhang, W. Zhong and Y. Dua, Effects of ultrasonic cavitation intensity on the



- efficient liquid-exfoliation of MoS<sub>2</sub> nanosheets, *RSC Adv.*, 2014, **4**(92), 50981–50987.
- 61 X. Yang, Z. Chen, J. Fang, Q. Yang, W. Zhao, X. Qian, C. Liu, D. Zhou, S. Tao and X. Liu, Efficient exfoliation to MoS<sub>2</sub> nanosheets by salt-assisted refluxing and ultrasonication with photocatalytic application, *Mater. Lett.*, 2019, **255**, 126596.
- 62 S. Parida, A. Mishra, J. Chen, J. Wang, A. Doble, C. B. Carter and A. M. Dongare, Vertically stacked 2H-1T dual-phase MoS<sub>2</sub> microstructures during lithium intercalation: a first principles study, *J. Am. Ceram. Soc.*, 2020, **103**(11), 6603–6614.
- 63 A. Ambrosi, Z. Sofer and M. Pumera, Lithium intercalation compound dramatically influences the electrochemical properties of exfoliated MoS<sub>2</sub>, *Small*, 2015, **11**(5), 605–612.
- 64 M. A. Islam, P. Serles, B. Kumral, P. G. Demingos, T. Qureshi, A. Meiyazhagan, A. B. Puthirath, M. S. B. Abdullah, S. R. Faysal, P. M. Ajayan, D. Panesar, C. V. Singh and T. Filleter, Exfoliation mechanisms of 2D materials and their applications, *Applied Physics Reviews*, 2022, **9**, 4.
- 65 N. Liu, P. Kim, J. H. Kim, J. H. Ye, S. Kim and C. J. Lee, Large-area atomically thin MoS<sub>2</sub> nanosheets prepared using electrochemical exfoliation, *ACS Nano*, 2014, **8**(7), 6902–6910.
- 66 P. Zhang, Sh. Yang, R. Pineda-Gómez, B. Ibarlucea, J. Ma, M. R. Lohe, T. F. Akbar, L. Baraban, G. Cuniberti and X. Feng, Electrochemically Exfoliated High-Quality 2H-MoS<sub>2</sub> for Multiflake Thin Film Flexible Biosensors, *Small*, 2019, **15**(23), 1901265.
- 67 V. Forsberg, R. Zhang, J. Bäckström, C. Dahlström, B. Andres, M. Norgren, M. Andersson, M. Hummelgård and H. Olin, Exfoliated MoS<sub>2</sub> in water without additives, *PLoS One*, 2016, **11**(4), e0154522.
- 68 H. Yu, H. Zhu, M. Dargusch and Y. Huang, A reliable and highly efficient exfoliation method for water-dispersible MoS<sub>2</sub> nanosheet, *J. Colloid Interface Sci.*, 2018, **514**, 642–647.
- 69 A. Gupta, V. Arunachalam and S. Vasudevan, Liquid-phase exfoliation of MoS<sub>2</sub> nanosheets: the critical role of trace water, *J. Phys. Chem. Lett.*, 2016, **7**(23), 4884–4890.
- 70 H. Maa, Sh. Ben, Z. Shenb, X. Zhangb, C. Wua, Sh. Liaoa and F. Ana, Investigating the exfoliation behavior of MoS<sub>2</sub> and graphite in water: A comparative study, *Appl. Surf. Sci.*, 2020, **512**, 145588.
- 71 P. Wu, Z. Liu and Z. Cheng, Ultrasound-Assisted Alkaline Solution Reflux for As-Exfoliated MoS<sub>2</sub> Nanosheets, *ACS Omega*, 2019, **4**(6), 9823–9827.
- 72 K. Manna, H. Huang, W. Li, Y. Ho and W. Chiang, Toward understanding the efficient exfoliation of layered materials by water-assisted cosolvent liquid-phase exfoliation, *Chem. Mater.*, 2016, **28**(21), 7586–7593.
- 73 Sh. Venkatram, C. Kim, A. Chandrasekaran and R. Ramprasad, Critical assessment of the Hildebrand and Hansen solubility parameters for polymers, *J. Chem. Inf. Model.*, 2019, **59**(10), 4188–4194.
- 74 H. Maa, Sh. Benc, Z. Shenb, X. Zhang, C. Wua, Sh. Liao and F. An, Investigating the exfoliation behavior of MoS<sub>2</sub> and graphite in water: A comparative study, *Appl. Surf. Sci.*, 2020, **512**, 145588.
- 75 L. Muscuso, S. Cravanzola, F. Cesano, D. Scarano and A. Zecchina, Optical, vibrational, and structural properties of MoS<sub>2</sub> nanoparticles obtained by exfoliation and fragmentation *via* ultrasound cavitation in isopropyl alcohol, *J. Phys. Chem. C*, 2015, **119**(7), 3791–3801.
- 76 L. Takcs, The historical development of mechanochemistry, *Chem. Soc. Rev.*, 2013, **42**(18), 7649–7659.
- 77 K. S. Novoselov, A. K. Geim, S. V. Morozov, D. Jiang, Y. Zhang, S. V. Dubonos, I. V. Grigorieva and A. A. Firsov, Electric field effect in atomically thin carbon films, *science*, 2004, **306**(5696), 666–669.
- 78 M. Yi and Z. Shen, A review on mechanical exfoliation for the scalable production of graphene, *J. Mater. Chem. A*, 2015, **3**(22), 11700–11715.
- 79 N. Khossossi, D. Singh, A. Ainane and R. Ahuja, Recent progress of defect chemistry on 2D materials for advanced battery anodes, *Chem.-Asian J.*, 2020, **15**(21), 3390–3404.
- 80 A. Tayyebi, N. Ogino, T. Hayashi and N. Komatsu, Size-controlled MoS<sub>2</sub> nanosheet through ball milling exfoliation: parameter optimization, structural characterization and electrocatalytic application, *Nanotechnology*, 2019, **31**(7), 075704.
- 81 R. Quirós-Ovies, M. Laborda, N. M. Sabanés, L. Martín-Pérez, S. M. Silva, E. Burzuri, V. Sebastian, E. M. Pérez and J. Santamaría, Microwave-Driven Exfoliation of Bulk 2H-MoS<sub>2</sub> after Acetonitrile Prewetting Produces Large-Area Ultrathin Flakes with Exceptionally High Yield, *ACS Nano*, 2023, **17**(6), 5984–5993.
- 82 W. Wu, J. Xu, X. Tang, P. Xie, X. Liu, J. Xu, H. Zhou, D. Zhang and T. Fan, Two-dimensional nanosheets by rapid and efficient microwave exfoliation of layered materials, *Chem. Mater.*, 2018, **30**(17), 5932–5940.
- 83 J. Yan, Y. Huang, X. Zhang, X. Gong, C. Chen, G. Nie, X. Liu, P. Liu, J. Yan, *et al.*, MoS<sub>2</sub>-decorated/integrated carbon fiber: phase engineering well-regulated microwave absorber, *Nano-Micro Lett.*, 2021, **13**(1), 114.
- 84 P. Mohammad-Andashti, Z. Ramezani, V. Zare-Shahabad and P. Torabi, Rapid and green synthesis of highly luminescent MoS<sub>2</sub> quantum dots *via* microwave exfoliation of MoS<sub>2</sub> powder and its application as a fluorescence probe for cortisol detection in human saliva, *Colloids Surf., A*, 2022, **647**, 129048.
- 85 R. Ameta, M. S. Solanki, S. Benjamin and S. C. A. Photocatalysis, in *Advanced Oxidation Processes for Waste Water Treatment*. Academic Press, 2018. pp. 135–175.
- 86 M. Khan, *Theoretical Concepts of Photocatalysis*, Elsevier Inc, 2023, ISBN 978-0-323-95191-3.
- 87 K. M. Reza, A. Kurny and F. Gulshan, Parameters affecting the photocatalytic degradation of dyes using TiO<sub>2</sub>: a review, *Appl. Water Sci.*, 2017, **7**, 1569–1578.
- 88 I. Kazeminezhad and A. Sadollahkhani, Influence of pH on the photocatalytic activity of ZnO nanoparticles, *J. Mater. Sci.: Mater. Electron.*, 2016, **27**, 4206–4215.





- 89 A. Enesca and L. Isac, The influence of light irradiation on the photocatalytic degradation of organic pollutants, *Materials*, 2020, **13**(11), 2494.
- 90 J. M. Herrmann, Photocatalysis fundamentals revisited to avoid several misconceptions, *Appl. Catal., B*, 2010, **99**(3–4), 461–468.
- 91 N. G. Asenjo, R. Santamaria, C. Blanco, M. Granda, P. Alvarez and R. Menendez, Correct use of the Langmuir–Hinshelwood equation for proving the absence of a synergy effect in the photocatalytic degradation of phenol on a suspended mixture of titania and activated carbon, *Carbon*, 2013, **55**, 62–69.
- 92 L. O. Amaral and A. L. Daniel-da-Silva, MoS<sub>2</sub> and MoS<sub>2</sub> Nanocomposites for Adsorption and Photodegradation of Water Pollutants: A Review, *Molecules*, 2022, **27**(20), 6782.
- 93 P. R. Sivaranjani, B. Janani, A. M. Thomas, L. L. Raju and S. Sudheer Khan, Recent development in MoS<sub>2</sub>-based nano-photocatalyst for the degradation of pharmaceutically active compounds, *J. Cleaner Prod.*, 2022, **352**, 131506.
- 94 A. Rahman, J. R. Jennings, A. L. Tan and M. M. Khan, Molybdenum disulfide-based nanomaterials for visible-light-induced photocatalysis, *ACS Omega*, 2022, **7**(26), 22089–22110.
- 95 A. Rahman and M. Khan, Chalcogenides as photocatalysts, *New J. Chem.*, 2021, **45**, 19622.
- 96 W. Zhang, X. Xiao, Y. L. X. Zeng, L. Zheng and C. Wan, Liquid-exfoliation of layered MoS<sub>2</sub> for enhancing photocatalytic activity of TiO<sub>2</sub>/g-C<sub>3</sub>N<sub>4</sub> photocatalyst and DFT study, *Appl. Surf. Sci.*, 2016, **389**, 496–506.
- 97 S. V. Kite, A. N. Kadam, D. J. Sathe, S. Patil, S. S. Mali, C. K. Hong, S. Lee and K. M. Garadkar, Nanostructured TiO<sub>2</sub> sensitized with MoS<sub>2</sub> nanoflowers for enhanced photodegradation efficiency toward methyl orange, *ACS Omega*, 2021, **6**(26), 17071–17085.
- 98 Q. Jiang, L. Sun, J. Bi, Sh. Liang, L. Li, Y. Yu and L. Wu, MoS<sub>2</sub> Quantum Dots-Modified Covalent Triazine-Based Frameworks for Enhanced Photocatalytic Hydrogen Evolution, *ChemSusChem*, 2018, **11**(6), 1108–1113.
- 99 H. Zhang, Q. Feng, F. Yu, Y. Wang, C. Liu, Q. Liu, L. Yin, J. Huang and X. Kong, MoS<sub>2</sub>-Modified CdS Hexagonal Pyramid To Form a New Photogenerated Carrier Migration Path with Highly Efficient Photocatalytic H<sub>2</sub> Performance, *J. Phys. Chem. C*, 2022, **126**(21), 9027–9033.
- 100 Sh. Singh, A. Modak, K. K. Pant, A. Sinhamahapatra and P. Biswas, MoS<sub>2</sub>-nanosheets-based catalysts for photocatalytic CO<sub>2</sub> reduction: A review, *ACS Appl. Nano Mater.*, 2021, **4**(9), 8644–8667.
- 101 H. Cho, *et al.*, Bandgap Engineering of MoS<sub>2</sub> for Visible Light-Induced Photocatalytic Activities: The Role of Tungsten Substitution, *Adv. Mater.*, 2016, **28**(19), 4053–4058.
- 102 X. Zhang, *et al.*, Heterostructures of MoS<sub>2</sub>/TiO<sub>2</sub> for Enhanced Photocatalytic Hydrogen Evolution: An In-Depth Study on Interface Engineering, *Chem. Mater.*, 2020, **32**(8), 3352–3361.
- 103 J. Kim, *et al.*, Engineered MoS<sub>2</sub> for Bimolecular Photocatalysis: Enhanced Activity for H<sub>2</sub> Evolution and Selective Generation of H<sub>2</sub>O<sub>2</sub>, *J. Am. Chem. Soc.*, 2017, **139**(19), 6829–6836.
- 104 W. Yin, *et al.*, Engineering the Coordination Environment of Single-Metal Sites to Improve Photocatalytic Performance, *Adv. Mater.*, 2017, **29**(9), 1606793.
- 105 H. Zhang, *et al.*, Controlled Synthesis of MoS<sub>2</sub> Nanosheets with Tunable Morphology and Enhanced Photocatalytic Activity, *Sci. Rep.*, 2016, **6**, 35102.
- 106 B. Tian, *et al.*, Modulation of the Particle Size and Shape of MoS<sub>2</sub> Nanosheets for Enhanced Photocatalytic Hydrogen Evolution, *J. Mater. Chem. A*, 2018, **6**(34), 16544–16549.
- 107 K. F. Mak, *et al.*, Atomically Thin MoS<sub>2</sub>: A New Direct-Gap Semiconductor, *Phys. Rev. Lett.*, 2012, **105**(13), 136805.
- 108 A. Lu, *et al.*, MoS<sub>2</sub>/Graphene Composite Anodes with Enhanced Performance for Sodium-Ion Batteries: The Role of the Two-Dimensional Heterointerface, *Adv. Energy Mater.*, 2015, **5**(21), 1500993.
- 109 Y. Fu, *et al.*, MoS<sub>2</sub>-Based Photocatalysis: The Intriguing Structures of MoS<sub>2</sub> and Its Applications in Degradation of Organic Pollutants, *ChemSusChem*, 2016, **9**(13), 1523–1544.
- 110 Y. Xue, *et al.*, MoS<sub>2</sub>/Ag<sub>3</sub>PO<sub>4</sub> Hybrid Nanocomposites for Enhanced Visible Light Photocatalysis: Mechanistic Insights and Antibacterial Activity, *Appl. Surf. Sci.*, 2019, **483**, 185–197.
- 111 Z. Zhao, *et al.*, A Hybrid Material of Graphene and MoS<sub>2</sub> Nanoparticles with Ultra-High Photoresponsive Nonlinear Optical Performance, *Adv. Funct. Mater.*, 2015, **25**(9), 1380–1388.
- 112 Y. Tian, *et al.*, MoS<sub>2</sub>/Carbon Nanotube Composite Anodes with Enhanced Performance for Lithium-Ion Batteries: The Role of Morphology and Synergy, *ChemElectroChem*, 2018, **5**(1), 79–88.

